Nucleon Elastic Form Factors Experiments and Data

Donal Day
University of Virginia

January 12, 2004

Outline

- Introduction, Motivation and Formalism
- Traditional Techniques and Data (pre-1998)
- Models
- Modern Experiments
  - Recoil Polarization
  - Beam-Target Asymmetry
  - Ratio method
  - Rosenbluth–Polarization Discrepancy
- Prospects and Conclusion

Nucleons have Structure!

Early Indications

- Anomalous magnetic moments of p and n
  O. Stern, Nature 132 (1933) 169
- Non-zero neutron charge radius from scattering of thermal neutrons on atoms
- Experiments on Nucleon Structure go back to the mid 1950's at Stanford, see *Nuclear and Nucleon Structure, R. Hofstader, W.A. Benjamin (1963).*

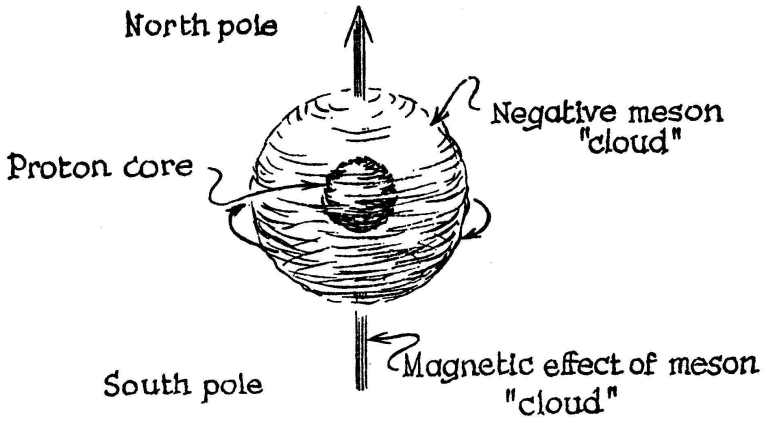

Motivation

- ✷ FF are fundamental quantities
- ✷ Describe the internal structure of the nucleon
- ✷ Provide rigorous tests of QCD description of the nucleon

  Symmetric quark model, with all valence quarks with same wf: $G_E^n \equiv 0$

  $G_E^n \neq 0 \rightarrow$ details of the wavefunctions
- ✷ Necessary for study of nuclear structure

  Few body structure functions

50 years of effort has produced much but $\cdots$ what is new?

- ✷ New techniques, unexpected behavior, and a reinvigorated theoretical effort have made the last decade one of dynamic progress.

The few body system is our best source of information about NN potential, FSI and MEC.

Quark spin-dependent interaction breaks the mass degeneracy of the ground state baryons also leads to a segregation of charge within the nucleon. If the perturbing force is more repulsive for quarks with parallel than antiparallel spins, the induced charge radius $< r^2 >_n$ will be negative.

Explains $\left\langle \mathbf{r}^{\mathbf{2}}_{\mathrm{ch}} \right\rangle$ of ^{48}Ca as compared to ^{40}Ca

Formalism

$$\frac{d\sigma}{d\Omega} = \sigma_{\text{Mott}} \frac{E'}{E_0} \left\{ (F_1)^2 + \tau \left[2 (F_1 + F_2)^2 \tan^2 (\theta_e) + (F_2)^2 \right] \right\}; F_{1,2} = F_{1,2}(Q^2)$$

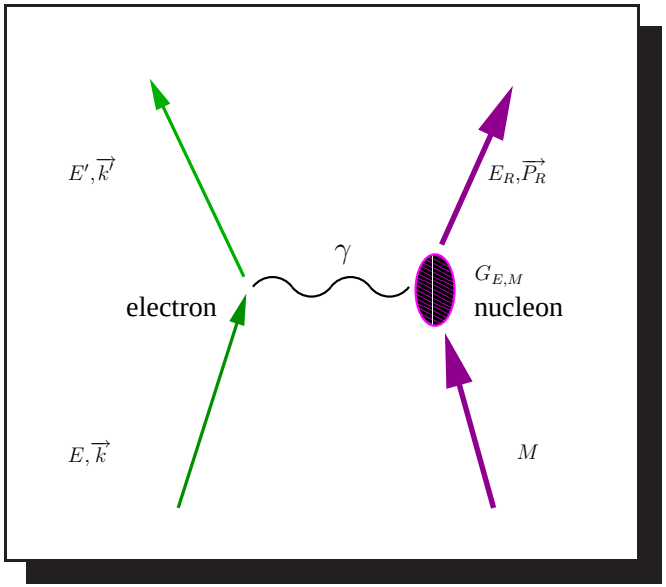

$Q^2 = 4EE' \sin^2(\theta/2)$	$\tau = \frac{Q^2}{4M^2}$
$F_1^p = 1$	$F_1^n = 0$
$F_2^p = 1.79$	$F_2^n = -1.91$

In Breit frame F_1 and F_2 related to charge and spatial curent densities:

$$\rho = J_0 = 2eM[F_1 - \tau F_2]$$

$$J_i = e\bar{u}\gamma_i u[F_1 + F_2]_{i=1,2,3}$$

$$G_E\left(Q^2\right) = F_1(Q^2) - \tau F_2\left(Q^2\right) \qquad G_M\left(Q^2\right) = F_1\left(Q^2\right) + F_2\left(Q^2\right)$$

✶ For a point like probe G_E and G_M are the FT of the charge and magnetizations distributions in the nucleon, with the following normalizations

$Q^2 = 0$ limit: $G_E^p = 1$ $G_E^n = 0$ $G_M^p = 2.79$ $G_M^n = -1.91$

Proton Form Factor Data (pre-1998)

Rosenbluth formula, Rosenlbuth separation:

$$\frac{d\sigma}{d\Omega} = \sigma_{\rm NS}\left[\frac{G_E^2+\tau G_M^2}{1+\tau} + 2\tau G_M^2\tan^2(\theta/2)\right] \qquad \tau = \frac{Q^2}{4M^2}$$

$$\Rightarrow \quad \sigma_R \equiv \frac{d\sigma}{d\Omega}\frac{\epsilon(1+\tau)}{\sigma_{\rm NS}} = \underbrace{\tau G_M^2(Q^2)}_{\text{intercept}} + \epsilon\underbrace{G_E^2(Q^2)}_{\text{slope}} \qquad \epsilon^{-1} = 1+2(1+\tau)\tan(\theta/2)^2$$

$$\underbrace{G_E^p(Q^2) \approx \frac{G_M^p(Q^2)}{\mu_p} \approx \frac{G_M^n(Q^2)}{\mu_n}}_{\text{Scaling Law}} \approx \underbrace{G_D \equiv \left(1+\frac{Q^2}{0.71}\right)^{-2}}_{\text{Dipole Law}}$$

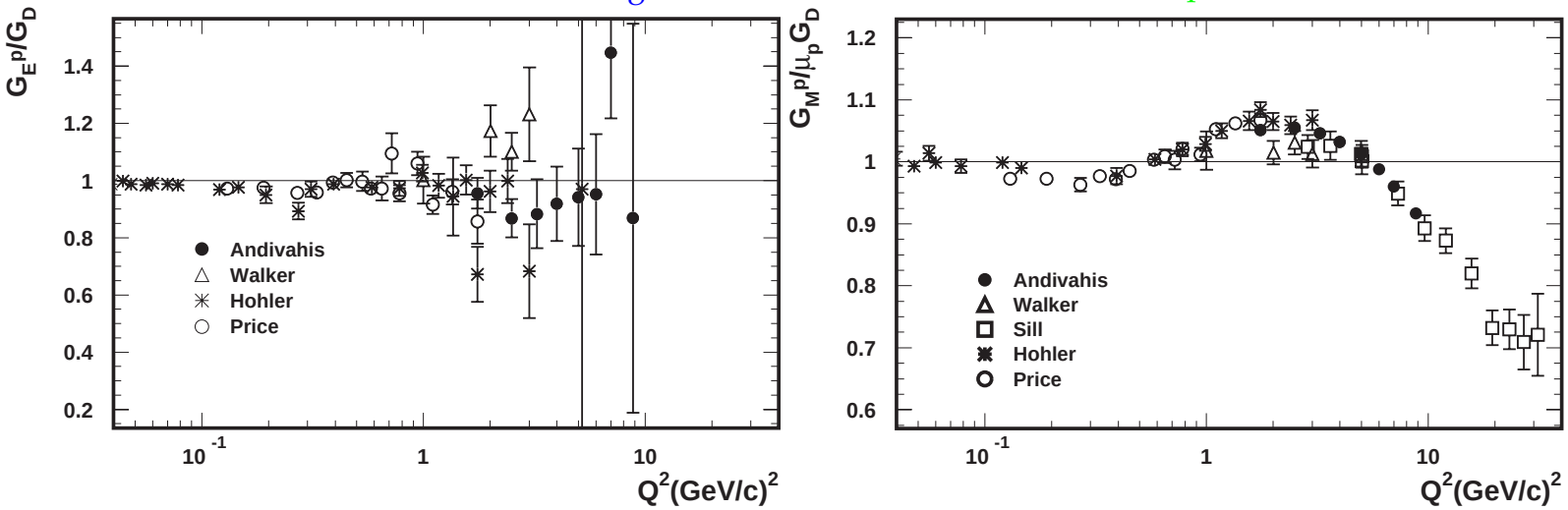

Notes

Exponential charge distribution, $\rho(r) = \rho_0 e^{-r/r_0}$, generates the dipole form and $G_D = \left(1 + \frac{Q^2}{0.71}\right)$ gives a rms radius of 0.81 fm

Plot of $\sigma_R \equiv \frac{d\sigma}{d\Omega}\frac{\epsilon(1+\tau)}{\sigma_{\rm NS}}$ taken at fixed Q^2 as a function of ϵ should be a straight line. The intercept of the line is $2\tau G_M^2$, while the slope is G_E^2. Errors in G_E and G_M are determined from the errors in the determination of the slope and intercept.

Linearity of the Rosenbluth formula is based on single photon exchange. As we shall see, this long held assumption is now being reexamined.

Scaling law and dipole scaling are good to 10% up to almost 10 GeV^2.

Traditional techniques to measure Neutron Form Factors

- No neutron target
- proton dominates neutron
- G_M^n dominates G_E^n

G_M^n and G_E^n measured through:

- Elastic scattering $^2\mathrm{H}(e,e')^2\mathrm{H}$
- Inclusive quasielastic scattering: $^2\mathrm{H}(e,e')X$
- Neutron in coincidence with electron: $^2\mathrm{H}(e,e'n)p$
- Ratio techniques $\frac{d(e,e'n)p}{d(e,e'p)n}$

Quasielastic kinematics and simplest nucleus

Notes

- ✷ Ratio techniques $\frac{d(e,e'n)p}{d(e,e'p)n}$ minimizes roles of g.s. wavefunction and FSI.

CLAS and G_M^n

G_M^n unpolarized

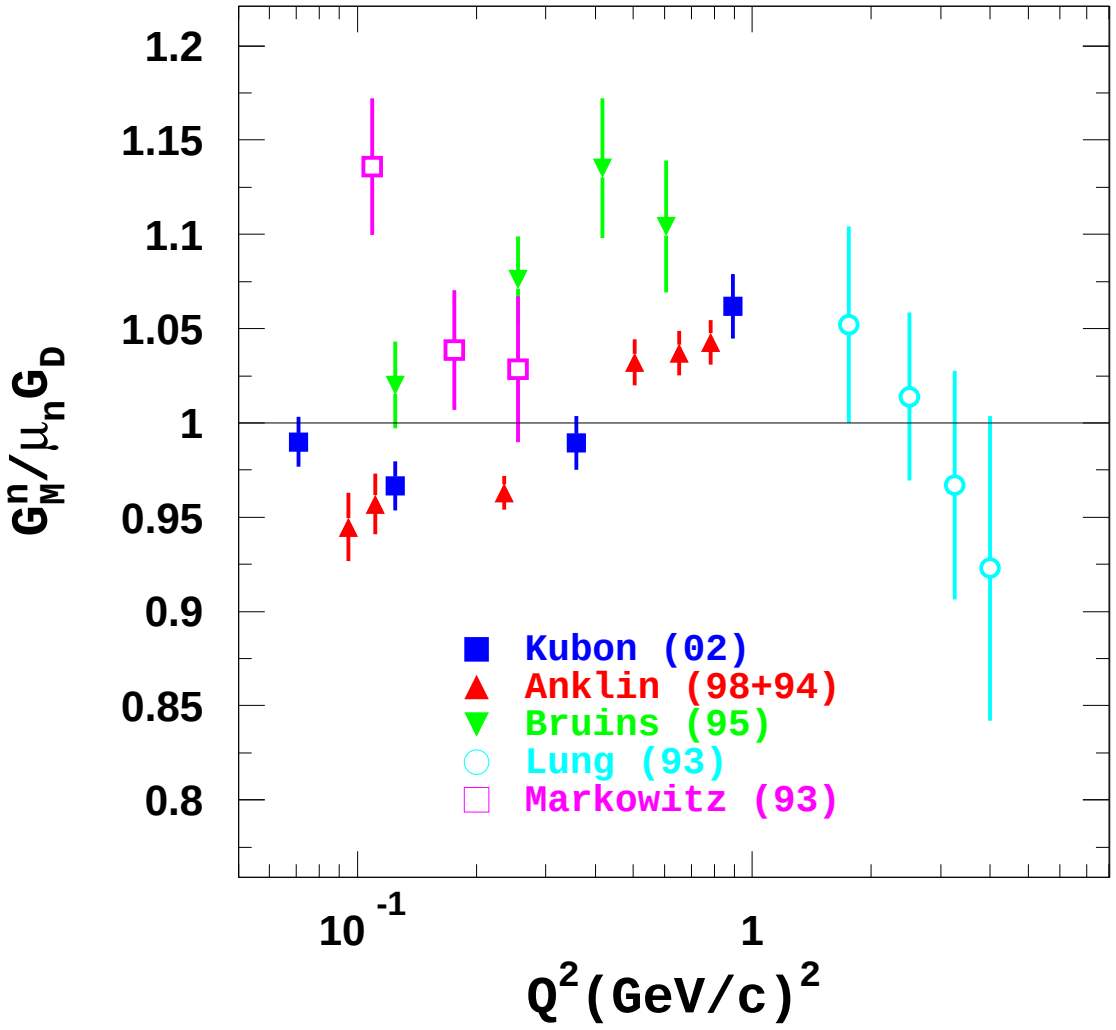

Kubon	ratio
Anklin	ratio
Bruins	ratio
Lung	$D(e,e')X$
Markowitz	$D(e,e'n)p$

$$\text{ratio} \equiv \frac{D(e,e'n)p}{D(e,e'p)n}$$

G_E^n through elastic $D(e, e')$

Extract from e-D elastic scattering:

$$\frac{d\sigma}{d\Omega} = \sigma_{NS} \left[A\left(Q^2\right) + B\left(Q^2\right) \tan^2\left(\frac{\theta_e}{2}\right) \right]$$

small θ_e approximation

$$\frac{d\sigma}{d\Omega} = \cdots (G_E^p + G_E^n)^2 \left[u(r)^2 + w(r)^2\right] j_0(\frac{qr}{2}) dr \cdots$$

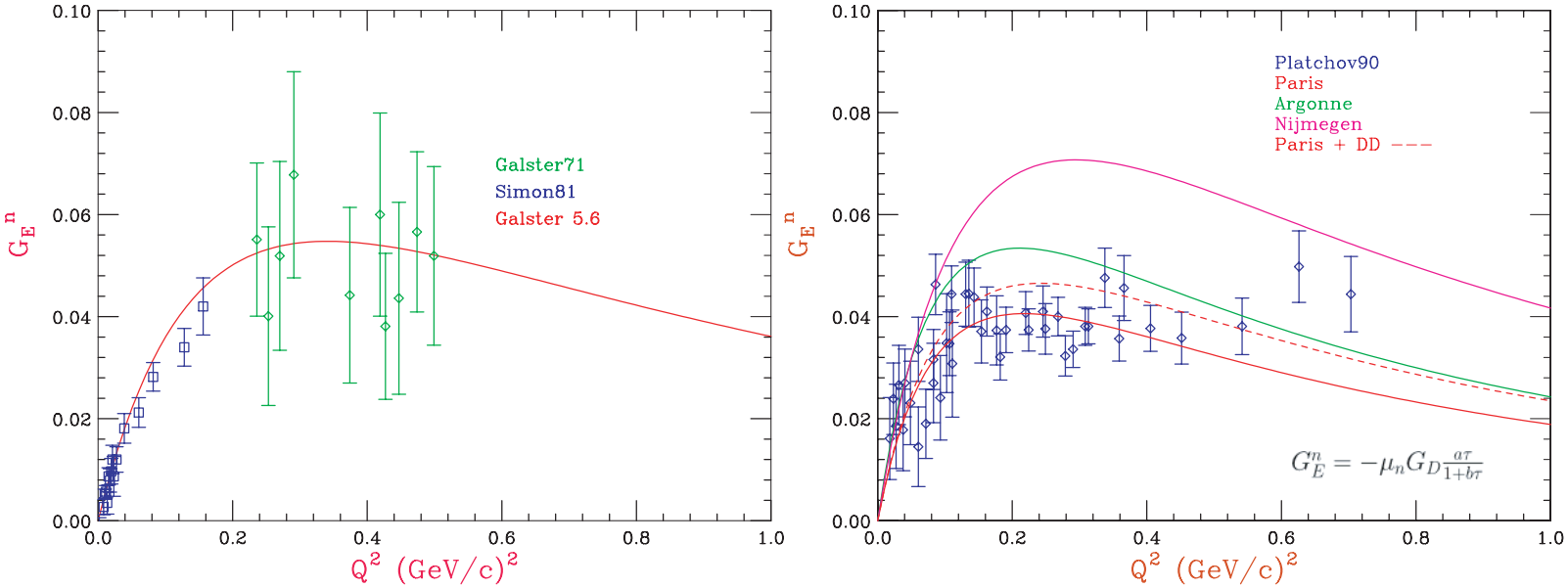

Galster Parametrization: $G_E^n = -\frac{\tau \mu_n}{1+5.6\tau} G_D$

Notes on eD

Elastic $e - D$ scattering at small angles

Neutron–proton interference a plus

Spin-1 ground state: three form factors, G_C , G_Q , G_M

$$A(Q^2) = G_c^2 + \tfrac{8}{9}\eta G_Q^2 + \tfrac{2}{3}\eta^2 G_M^2 \qquad B(Q^2) = \tfrac{4}{3}\eta(\eta+1)G_M^2$$

$$\eta = \frac{Q^2}{4M_D^2}$$

$A_{\rm IA}(Q^2)$ (sum of proton and neutron responses with deuteron wavefunction weighting) deduced after corrections for relativistic effects and MEC

Subtract magnetic dipole using parametrization of data

S and D state functions to unfold nuclear structure for various potentials to get isoscalar form factor

Subtract proton form factor to get G_E^n

Sensitive to deuteron wavefunction model and MEC

G_E^n from Elastic Scattering – D$(e, e'\vec{\mathrm{d}})$

Components of the tensor polarization give useful combinations of the form factors,

$$t_{20} = \frac{1}{\sqrt{2}S}\left\{\frac{8}{3}\tau_d G_C G_Q + \frac{8}{9}\tau_d^2 G_Q^2 + \frac{1}{3}\tau_d\left[1 + 2(1+\tau_d)\tan^2(\theta/2)\right]G_M^2\right\}$$

allowing $G_Q(Q^2)$ to be extracted. Exploiting the fact that $G_Q(Q^2) = (G_E^p + G_E^n)C_Q(q)$ suffers less from theoretical uncertainties than $A(Q^2)$, G_E^n can be extracted to larger momentum transfers.

E94-018!!

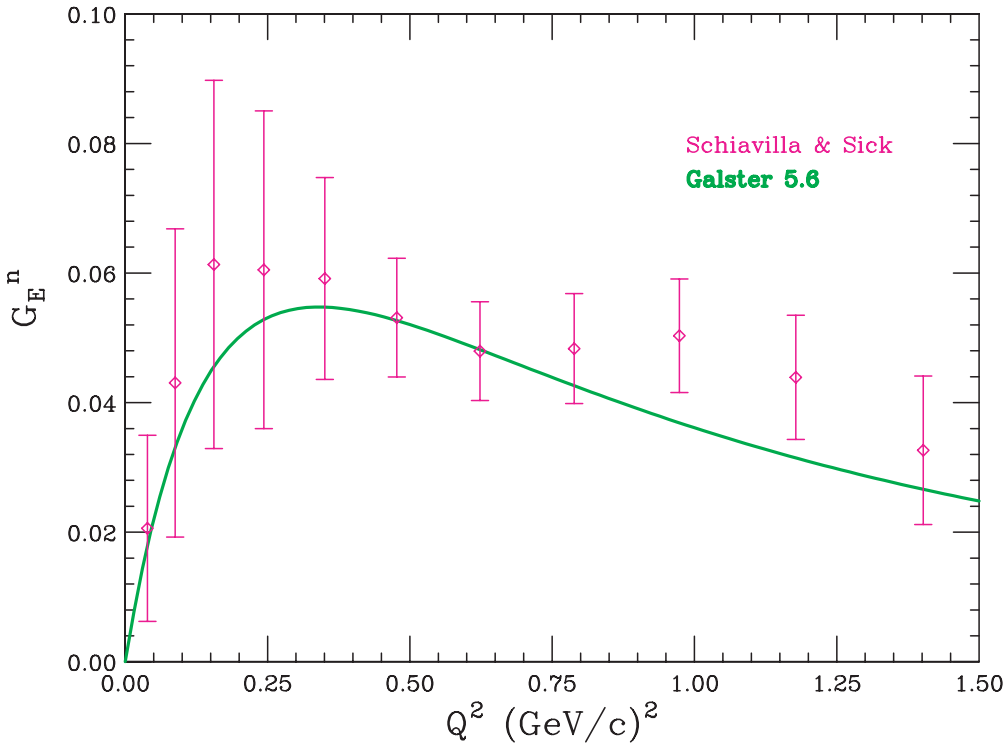

Notes T20: Why $G_C(q)$ is less sensitive to theory then $G_E(q)$.

Compare:

$$C_Q(q) = \cdots (G_E^p + G_E^n)^2 \int w(r) \left[u(r) - \frac{w(r)}{2\sqrt{2}} \right] j_2(\frac{qr}{2}) dr$$

$$C_C(q) = \cdots (G_E^p + G_E^n)^2 \int \left[u(r)^2 + w(r)^2 \right] j_0(\frac{qr}{2}) dr$$

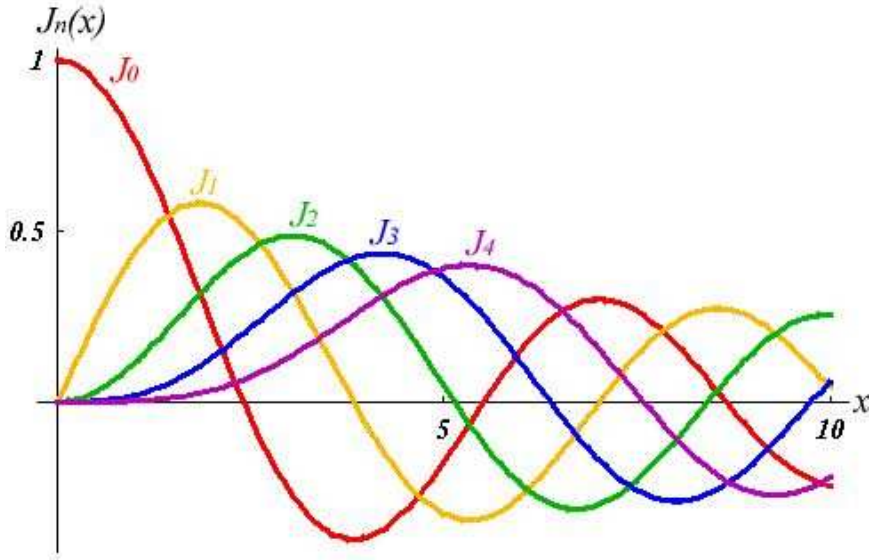

G_E^n at large Q^2 through $^2\mathrm{H}(e,e')X$

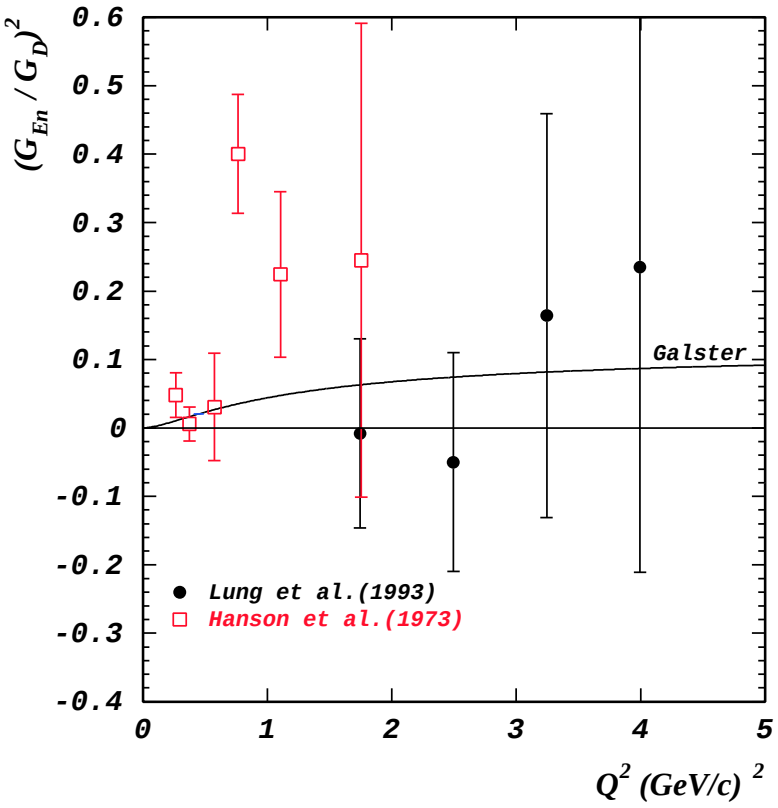

PWIA model σ is incoherent sum of p and n cross section folded with deuteron structure.

$$\begin{aligned}\sigma &= (\sigma_p + \sigma_n)\, I\,(u,w) \\ &= \varepsilon R_L + R_T\end{aligned}$$

- Extraction of G_E^n:
  Rosenbluth Separation $\Rightarrow R_L$
  Subtraction of proton contribution
- Problems:
  Unfavorable error propagation
  Sensitivity to deuteron structure

SLAC: *A. Lung et al, PRL. 70, 718 (1993)*

→No indication of non-zero G_E^n

Notes on Quasielastic

Can not get the sign of G_E^n from quasielastic,

$$\begin{aligned}
\sigma &= (\sigma_p + \sigma_n)\, I\,(u, w) \\
&= \left\{ \varepsilon \left[(G_E^p)^2 + (G_E^n)^2 \right] + \frac{\nu^2}{Q^2} \left[(G_M^p)^2 + (G_M^n)^2 \right] \right\} I\,(u, w) \\
&= \varepsilon R_L + R_T
\end{aligned}$$

$$\varepsilon = \left[1 + 2\,(1+\tau) \tan^2\,(\theta_e/2) \right]^{-1}$$

Open questions

$$\boxed{G_E\left(Q^2\right) = F_1(Q^2) - \tau F_2\left(Q^2\right) \qquad G_M\left(Q^2\right) = F_1\left(Q^2\right) + F_2\left(Q^2\right)}$$

If G_E^n is small at large Q^2 then F_1^n must cancel τF_2^n, begging the question, how does F_1^n evolve from 0 at $Q^2 = 0$ to cancel τF_2^n at large Q^2?

Models of Nucleon Form Factors

Dispersion relations

Formalism is model independent

$$F(t) = \frac{1}{\pi} \int_{t_0} \frac{\mathrm{Im} F(t')}{t' - t} dt'$$

Hoehler (1976), Hammer, Mergell, Meissner, Drechsel. Imaginary part of the spectral function receive contributions from all the possible intermediate states. Modeling is still necessary.

VMD

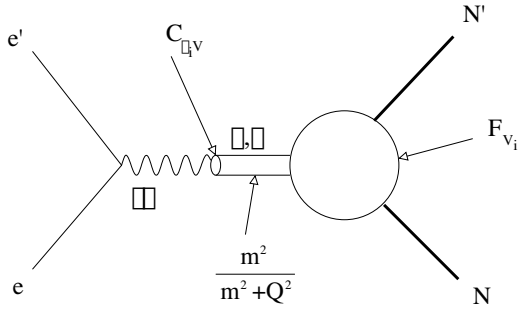

$$F(Q^2) = \sum_i \frac{C_{\gamma V_i}}{Q^2 + M^2_{V_i}} F_{V_i N}(Q^2)$$

Gari, Krumpelmann
Spectral function is approximated by a series of poles corresponding to vector mesons, ω, ϕ, and ρ appearing along the real axis. Fails to reproduce the large Q^2 behavior of pQCD.

---

pQCD

$$F_2 \propto F_1 \left(\frac{M}{Q^2} \right)$$

$$F_1 \propto \frac{\alpha_s^2(Q^2)}{Q^4}$$

$$Q^2 \frac{F_2}{F_1} \rightarrow \text{constant}$$

Farrar&Jackson, Brodksy&Lepage
Helicity conservation
Counting rules

JLAB data: $Q \frac{F_2}{F_1} \rightarrow$ constant

Models of Nucleon Form Factors

VMD-pQCD	At low Q^2 $F_1 \sim F_2 \sim \frac{\Lambda_1^2}{\Lambda_1^2+Q^2}$ with $\Lambda_1 \sim 0.8$ GeV At large Q^2 $F_1 \sim \left[\frac{1}{Q^2 \log(Q^2/\Lambda^2_{\rm QCD})}\right]$ $F_2 \sim \frac{F_1}{Q^2}$	Gari & Krumpelmann, Lomon Failure to follow the high Q^2 behavior suggested by pQCD led GK to incorporate pQCD at high Q^2 with the low VMD behavior. Inclusion of ϕ by GK had significant effect on G_E^n. Lomon has updated with new fits to selected data.
Lattice	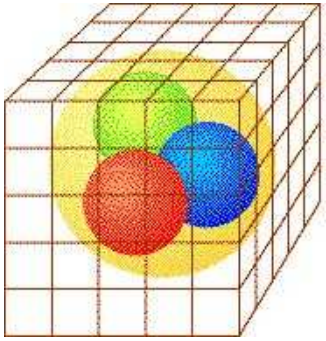	Dong, Liu, &Williams; Thomas.... Limitations in computer speed; quark masses 5-10 times higher than the physical values; quenched QCD
RCQM	light front point form	Miller.., Cardarelli & Simula CM motion and relative motion of quarks separated, SU(6) symmetry breaking by Melosh rotations Wagenbrunn... PFSA, GBE

Models of Nucleon Form Factors

CBM	$\mathcal{L}_{\rm CBM} \cong \mathcal{L}_{\rm MITBag} + \mathcal{L}_{\rm Free-\pi} + \mathcal{L}_{\rm int}$	Lu, Thomas, Williams
LFCBM	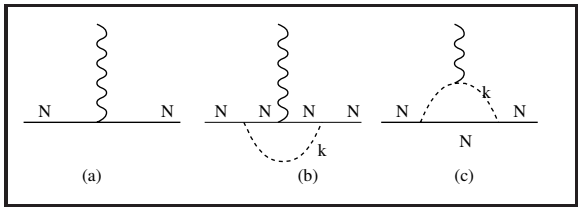	Miller
Helicity	Helicity non-conservation through Quark orbital angular momentum	Ralston.. (pQCD) Miller...(RCQM) Brodsky

Lattice–Quenched QCD Ever since the pioneering numerical simulations of lattice QCD in 1981, the calculation of the light hadron spectrum has been a fundamental subject in lattice QCD. QCD simulations on the lattice, however, require a huge amount of computer time. Therefore, most large scale simulations have been performed using an approximation of neglecting the effects of quark pair-creations and annihilations in the vacuum (quenched approximation). This reduces the computer time by a factor more than 100 and enables QCD simulations on relatively large lattices with high statistics.

Extrapolation of quark massess incorporate the constraints of chiral symmetry

Hank Thacker Donal: Most, if not all, of the calculations of nucleon form factors to date have used what are called Wilson or Wilson-Dirac fermions. This refers to the particular way of discretising the Dirac opeator for quarks on the lattice. The up and down quark masses have a mass of about 4 and 7 MeV respectively, using standard conventions. Wilson fermions work very well for quark masses greater than about 40 or 50 MeV, but by the time you get down to about 30 MeV, the statistics suddenly go all to hell from what is called the "exceptional configuration problem." My collaborators (Bardeen, Duncan, and Eichten) and I were the first ones to diagnose this problem and implement a cure for it. In our recent work, we have been able to get down to quark masses of about 15 to 20 MeV. But up till now, all of our calculations have been focused on chiral symmetry and, specifically, properties of scalar and pseudoscalar mesons. Also, there have been some relatively recent theoretical developments regarding how to put very light quarks on a lattice (keywords: overlap Dirac operator, Ginsparg-Wilson relations). Future calculations of nucleon form factors will certainly use these new light-quark methods and hopefully get much closer to the physical quark masses. There is also an extensive amount of theoretical work on the general problem of "chiral extrapolation", i.e. understanding from a chiral Lagrangian framework how various quantities depend on the quark mass so we can do more believable extrapolations to the physical values. The state of the art in the whole subject of light quark properties in lattice QCD is a rapidly developing subject. Most of the new technology has not been applied to nucleon form factors yet, so vastly improved calculations will certainly be forthcoming. I myself have been focusing more on mesons recently (which are simpler and more directly relevant to chiral symmetry), but baryon structure will certainly be studied at much lighter quark masses in the relatively near future. –Hank

VMD-PQCD: Eq 2 from GK (1085)

$$F_1^{IV} = \left[\frac{m_\rho^2}{m_\rho^2 + Q^2} \frac{g_\rho}{f_\rho} + \left(1 - \frac{g_\rho}{f_\rho} \right) \right] F_1(Q^2)$$

F1,F2 at low Q2 are known from meson physics and have the monopole form. Due to the additonal pwer of q2 in meson propagator it dies out and we are left with the photon nucleon coupling.

Theoretical Models

Vector Meson Dominance

Interaction in terms of coupling strengths of virtual photon and vector mesons and vector mesons and nucleon. Success at low and moderate Q^2 offset by failure to accomodate pQCD.

pQCD

High Q^2 helicity conservation requires that $Q^2 F_1/F_2 \rightarrow$ constant as F_2 helicity flip arises from second order corrections and are suppressed by an additional factor of $1/Q$. Furthermore for $Q^2 \gg \Lambda_{QCD}$ counting rules find $F_1 \propto \alpha_s(Q^2)/Q^4$. Thus $F_1 \propto \frac{1}{Q^4}$ and $F_2 \propto \frac{1}{Q^6} \Rightarrow Q^2 \frac{F_2}{F_1} \rightarrow$ constant.

Lattice calculations of form form factors

Fundamental but limited in stat. accuracy

Dong *et al* PRD58, 074504 (1998)

QCD based Models

Try to capture aspects of QCD

RCQM, Di-quark model, CBM

Hybrid Models

Failure to follow the high Q^2 behavior suggested by pQCD led GK to incorporate pQCD at high Q^2 with the low VMD behavior. Inclusion of ϕ by GK had significant effect on G_E^n. Lomon has updated with new fits to selected data.

Helicity non-conservation shows up in the light front dynamics analysis of Miller which predicted $Q\frac{F_2}{F_1} \rightarrow$ constant and the violation of helicity conservation. Ralston's pQCD model also predicts that $Q\frac{F_2}{F_1} \rightarrow$ constant. Both models include quark orbital angular momentum.

Models of Nucleon Form Factors

VMD	$F(Q^2) = \sum_i \frac{C_{\gamma V_i}}{Q^2 + M_{V_i}^2} F_{V_i N}(Q^2)$
	breaks down at large Q^2
CBM	Lu, Thomas, Williams (1998)
pQCD	$F_2 \propto F_1 \left(\frac{M}{Q^2}\right)$ helicity conservation
	Counting rules: $F_1 \propto \frac{\alpha_s^2(Q^2)}{Q^4}$
	$Q^2 F_2/F_1 \rightarrow$ constant
	JLAB proton data: $Q F_2/F_1 \rightarrow$ constant
Hybrid VMD-pQCD	GK, Lomon
Lattice	Dong .. (1998)
RCQM	point form (Wagenbrunn..)
	light front (Cardarelli ..)
Soliton	Holzwarth
LFCBM	Miller
Helicity non-conservation	pQCD (Ralston..) LF (Miller..)

Theoretical Models

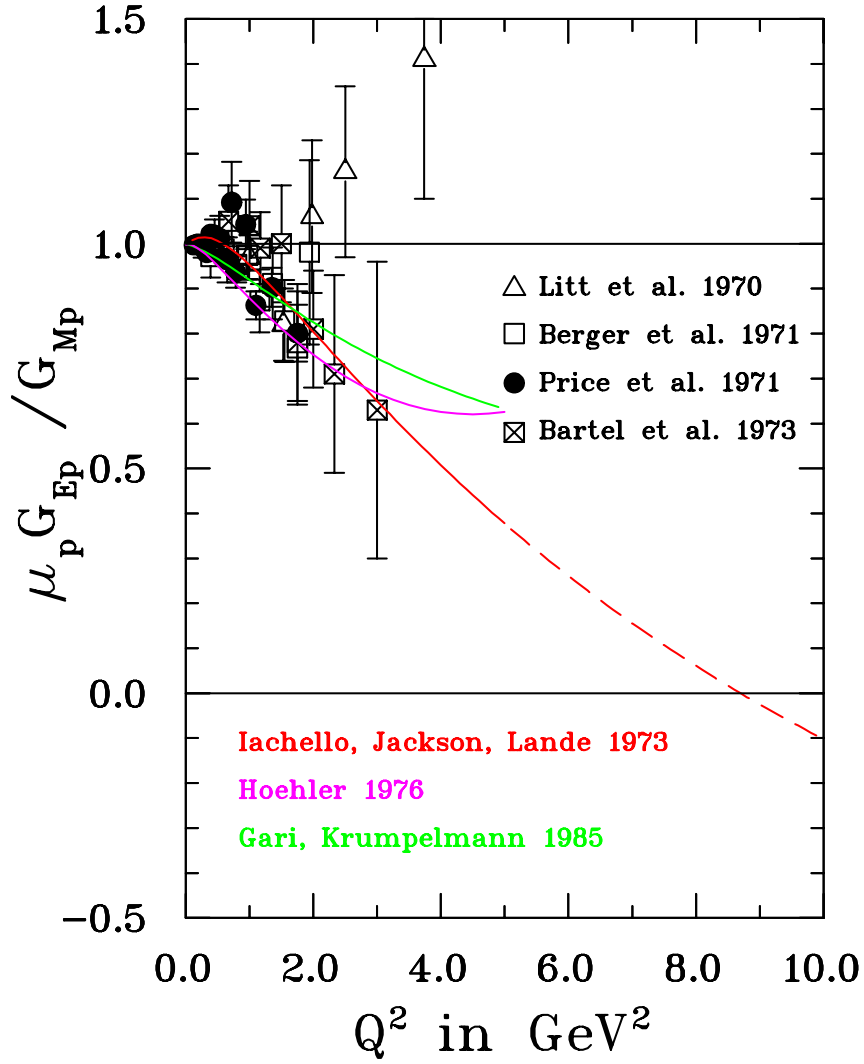

gepgmp jlab vsth early 11/11/02

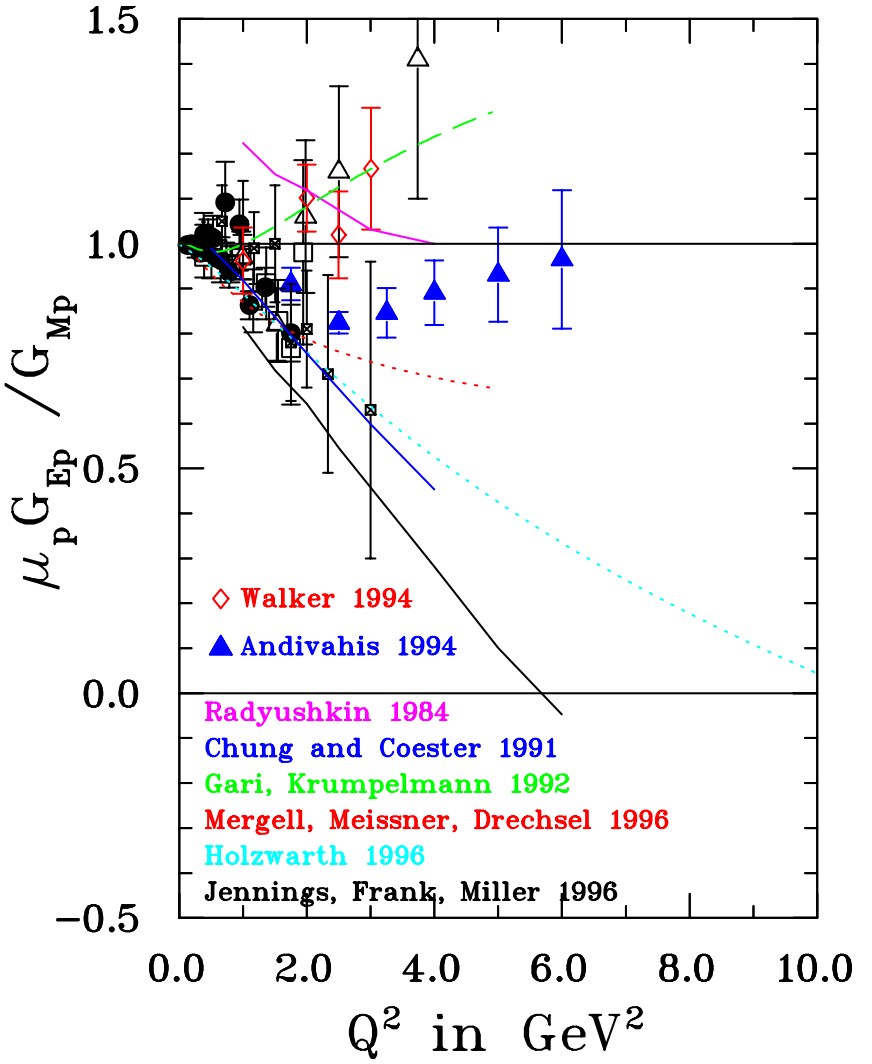

gepgmp jlab vsth prior 11/07/02

Theoretical Models

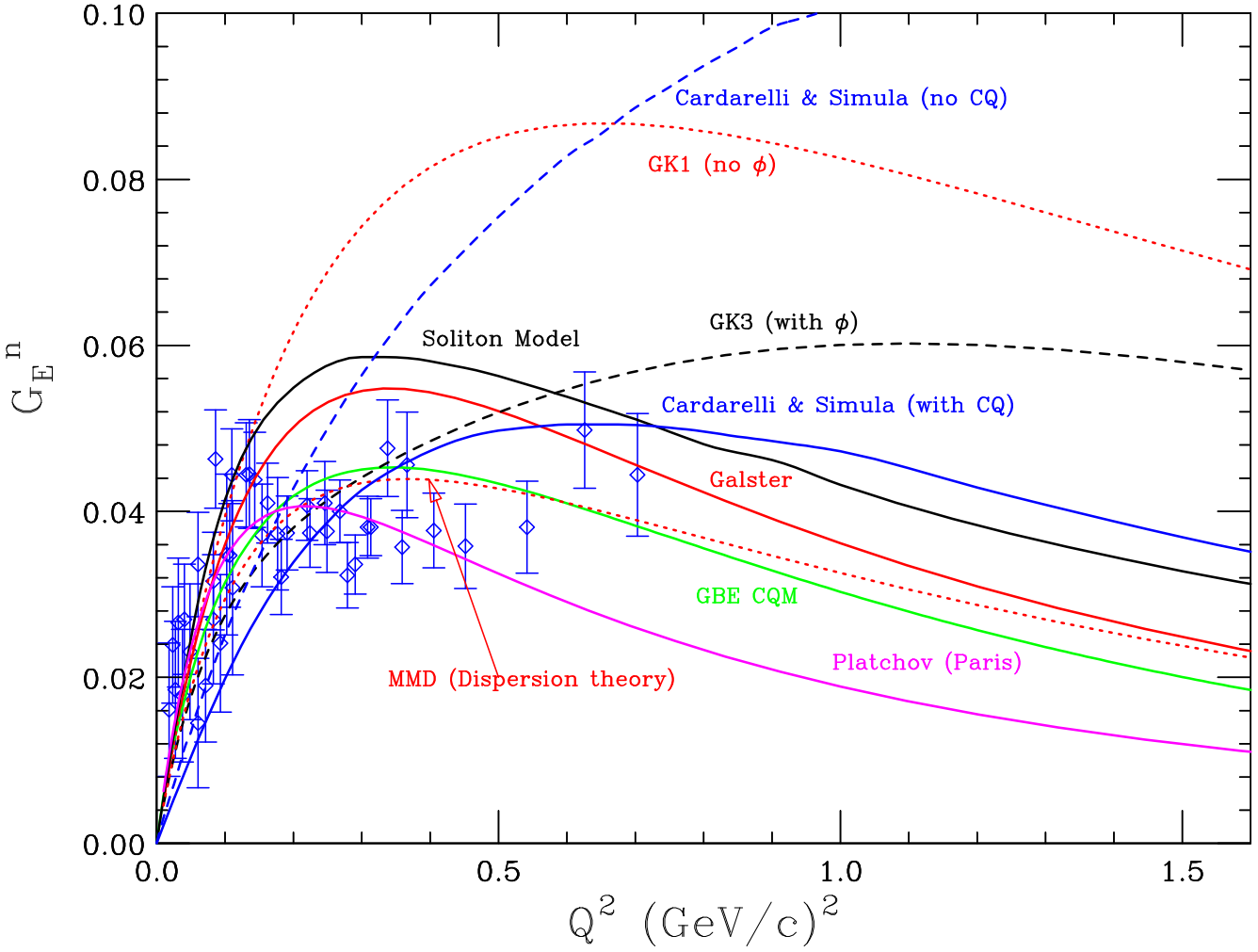

Spin Correlations in elastic scattering

- Dombey, Rev. Mod. Phys. **41** 236 (1968): $\vec{p}(\vec{e},e')$
- Akheizer and Rekalo, Sov. Phys. Doklady **13** 572 (1968): $p(\vec{e},e',\vec{p})$
- Arnold, Carlson and Gross, Phys. Rev. C **23** 363 (1981): $^2\mathrm{H}(\vec{e},e'\vec{n})p$

Early work at Bates, Mainz

- $^2\mathrm{H}(\vec{e},e'\vec{n})p$, Eden *et al.* (1994)
- $^1\mathrm{H}(\vec{e},e'\vec{p})$, Milbrath *et al.* (1998)
- $^3\overrightarrow{\mathrm{He}}(\vec{e},e')$, Woodward, Jones, Thompson, Gao (1990 - 1994)
- $^3\overrightarrow{\mathrm{He}}(\vec{e},e'n)$, Meyerhoff, (1994)

Essential feature:

$$\frac{d\sigma}{d\Omega} = \underbrace{\ldots(G_E^2+\ldots G_M^2)}_{(d\sigma/d\Omega)_{\mathrm{unpol}}} + \underbrace{\ldots P_e P_N^{\perp} G_E G_M}_{A_T} + \underbrace{\ldots P_e P_N^{\parallel} G_M^2}_{A_{\parallel}}$$

- Scofield, Phys. Rev. **141** 1352 (1966): all
- Dombey, Rev. Mod. Phys. **41** 236 (1968): $\vec{p}(\vec{e},\, e')$
- Akheizer and Rekalo, Sov. Phys. Doklady **13** 572 (1968): $p(\vec{e},\, e',\, \vec{p})$
- Hey and Kabir, Phys. Rev. **187** 1990 (1969): $\vec{p}(e,\, e',\, \vec{p})$
- Arnold, Carlson and Gross, Phys. Rev. C **23** 363 (1981): $^2\mathrm{H}(\vec{e},\, e'\vec{n})p$
- Blankleider and Woloshyn, Phys. Rev. C **29**, 538 (1984), polarized ^{3}He as an effective polarized neutron
- Arenhoevel, Leidemann and Tomusiak, Z. Phys. A 331 123 (1988), Polarization Observables in $d(e,\, e'n)p$

Polarization Experiments on the Neutron

Laboratory	Collaboration	$Q^2(GeV/c)^2$	Reaction	Reported
MIT-Bates	E85-05	0.255	$^2H(\tilde{e},e'\tilde{n})$	1994
Mainz-MAMI	A3	0.31	$^3\tilde{H}e(\tilde{e},e'n)$	1994
	A3	0.15, 0.34	$^2H(\tilde{e},e'\tilde{n})$	1999
	A3	0.385	$^3\tilde{H}e(\tilde{e},e'n)$	1999
	A1	0.67	$^3\tilde{H}e(\tilde{e},e'n)$	1999/2003
	A1	0.3, 0.6, 0.8	$^2H(\tilde{e},e'\tilde{n})$	in 2004
NIKHEF		0.21	$^2\tilde{H}(\tilde{e},e'n)$	1999
Jefferson Lab	E93026	0.5, 1.0	$^2\tilde{H}(\tilde{e},e'n)$	2001/2004
	E93038	0.45, 1.15, 1.47	$^2H(\tilde{e},e'\tilde{n})$	2003

Nucleon Form Factors

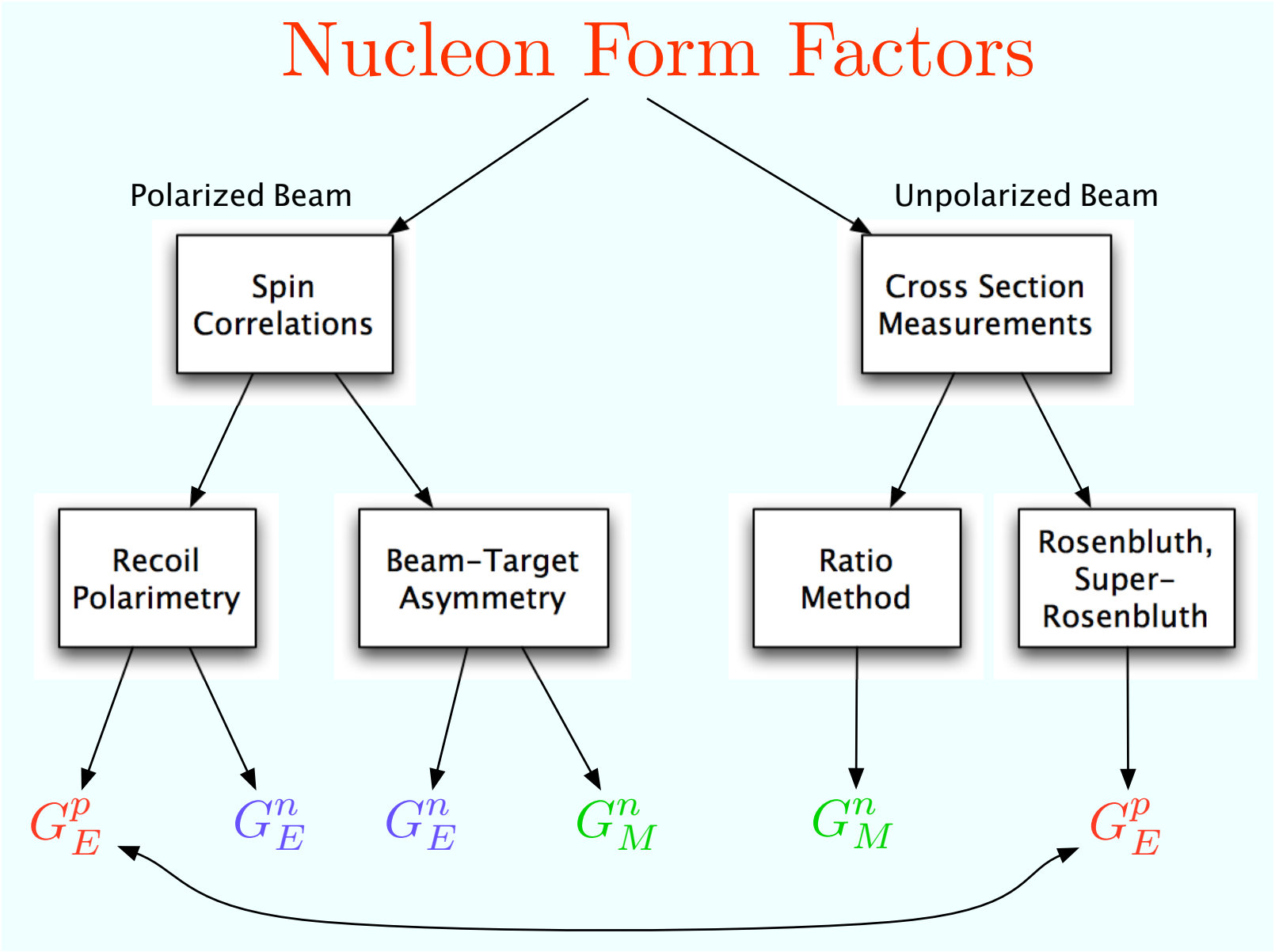

Recoil Polarization

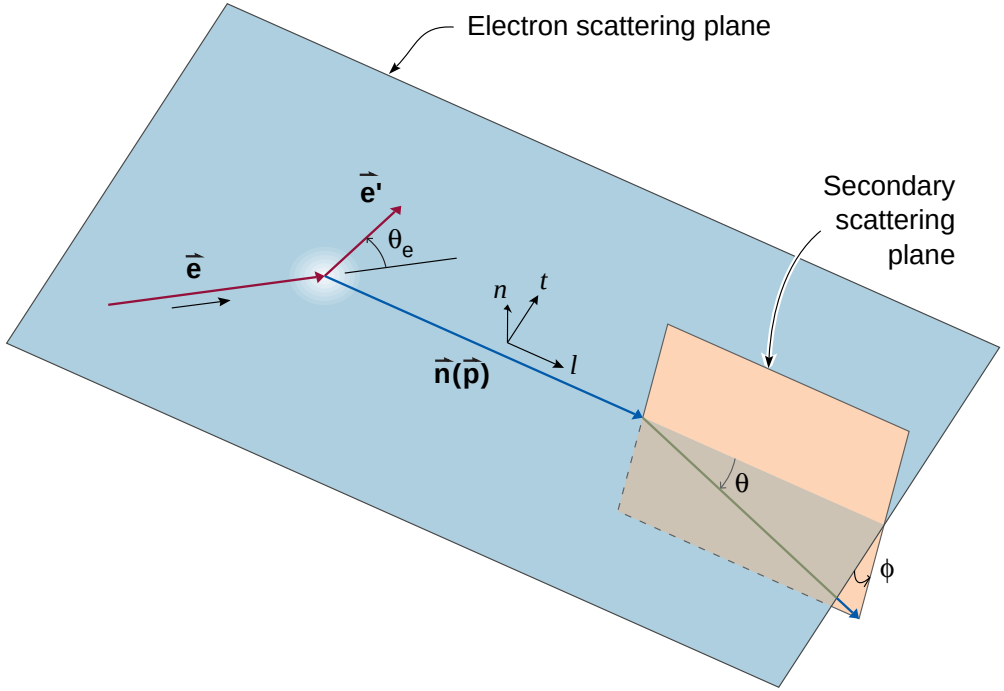

$$I_0 P_t = -2\sqrt{\tau(1+\tau)}\, G_E G_M \tan(\theta_e/2)$$

$$I_0 P_l = \frac{1}{M_N}(E_e + E_{e'})\sqrt{\tau(1+\tau)}\, G_M^2 \tan^2(\theta_e/2)$$

$$\frac{G_E}{G_M} = -\frac{P_t}{P_l}\frac{(E_e+E_{e'})}{2M_N}\tan\left(\frac{\theta_e}{2}\right)$$

Direct measurement of form factor ratio by measuring the ratio of the transfered polarization P_t and P_l

In elastic scattering of polarized electrons from a nucleon, the recoil nucleon obtains P_l and P_t sensitive to $G_E \cdot G_M$ and G_M^2 respectively.

Elastic scattering of polarised nucleons on unpolarised protons has analysing power $\epsilon(\theta_n)$ due to spin-orbit term V_{LS} in NN interaction:

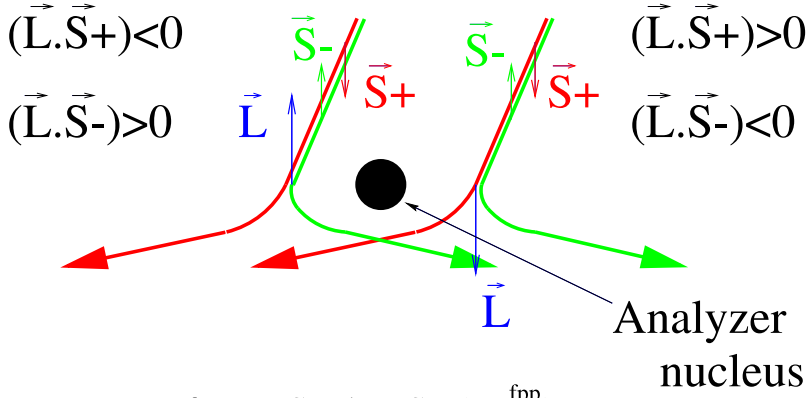

If more S+ than S- ($+P^{fpp}$) ...

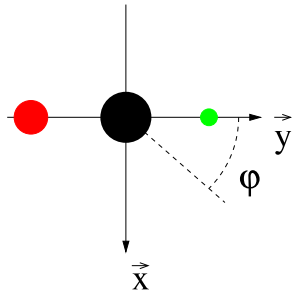

... more events left than right

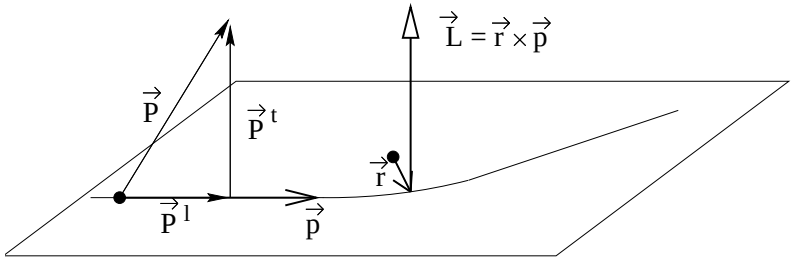

Left-right asymmetry is observed if the proton is polarized vertically, strong interaction with analyzer nucleus depends on its spin.

Recoil Polarization – Principle and Practice

- Interested in transfered polarization, P_l and P_t, at the target
- Polarimeters are sensitive to the perpendicular components only, P_n^{pol} and P_t^{pol}

  Measuring the ratio P_t/P_l requires the precession of P_l by angle χ before the polarimeter.
- If polarization precesses χ (e.g. in a dipole):
  $P_n^{\text{pol}} = \sin\chi \cdot hP_l$ and $P_t^{\text{pol}} = hP_t$

  $P_t^{\text{pol}} = P_t$ in scattering plane and proportional to $G_E G_M$

  P_n^{pol} is related to G_M^2
- G_E^p/G_M^p via $^1\text{H}(\vec{e}, e'\vec{p})$ at Jefferson Lab and Mainz
- G_E^n/G_M^n via $^2\text{H}(\vec{e}, e'\vec{n})p$ at Jefferson Lab and Mainz

Quality of polarimeter data optimized by taking advantage of proper flips (helicity reversals).

$$L_1 = N_o[1 + pA_y(\theta + \alpha)]$$
$$R_2 = N_o[1 - pA_y(\theta + \beta)]$$
$$R_1 = N_o[1 - pA_y(\theta + \alpha)]$$
$$L_2 = N_o[1 + pA_y(\theta + \beta)]$$

Using the geometric means, $L \equiv \sqrt{L_1 L_2}$and$R \equiv \sqrt{R_1 R_2}$, the false (instrumental) asymmetries, α and β, cancel.

$$\xi = pA_y = \frac{L - R}{L + R}$$

G_E^p in Hall A

E93-027 (data taken in 1998)

Jones *et al.*, PRL 84, 1398 (2000)

- G_E^p/G_M^p out to $Q^2 = 3.5$ GeV/c^2
- Electron in one HRS and proton in FPP in other HRS

E99-007 (data taken in 2000)

Gayou *et al.* PRL 88, 092301 (2002)

- G_E^p/G_M^p out to $Q^2 = 5.6$ GeV/c^2
- electron in one HRS and proton in FPP in other HRS
- above $Q^2 = 3.5$ proton in FPP in one HRS and electron in calorimeter.

G_E^p in Hall A

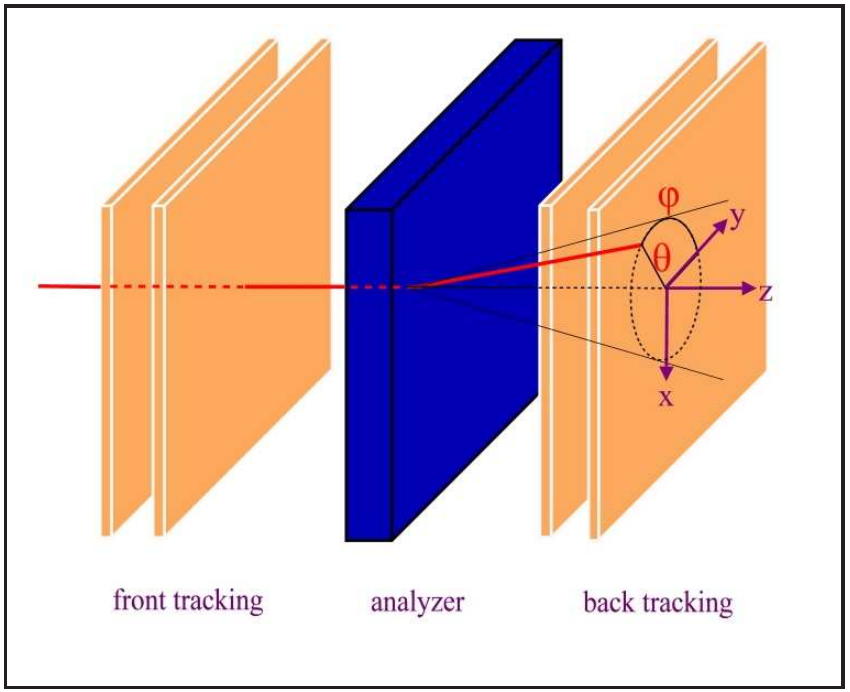

- left–right asymmetry $\Rightarrow P_n^{\text{fpp}}$ polarization in vertical direction
- up–down asymmetry $\Rightarrow P_t^{\text{fpp}}$ polarization in the horizontal direction

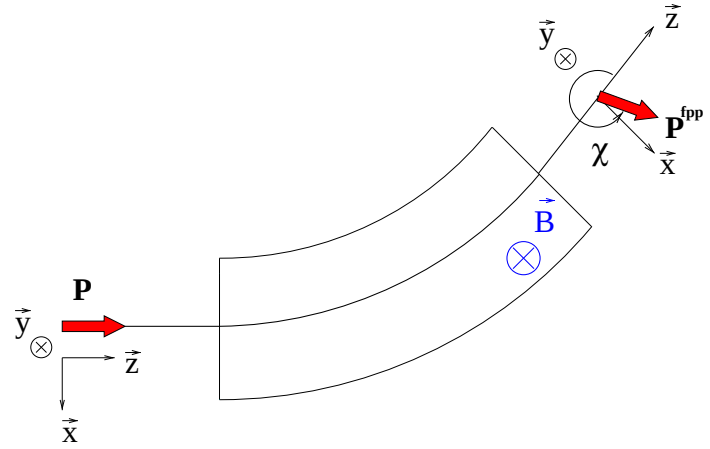

$$P_n^{\text{fpp}} = \sin\chi \cdot hP_l$$
$$P_t^{\text{fpp}} = hP_t$$
$$\chi = \gamma\theta_B(\mu_p - 1)$$

G_E^p in Hall A

Azimuthal Distribution

$$N(\vartheta,\varphi) = N_0(\vartheta)\epsilon(\vartheta)\left\{1 + \left[hA_y(\vartheta)P_t^{\text{fpp}} + a_{\text{instr}}\right]\sin\varphi - \left[hA_y(\vartheta)P_n^{\text{fpp}} + b_{\text{instr}}\right]\cos\varphi\right\}$$

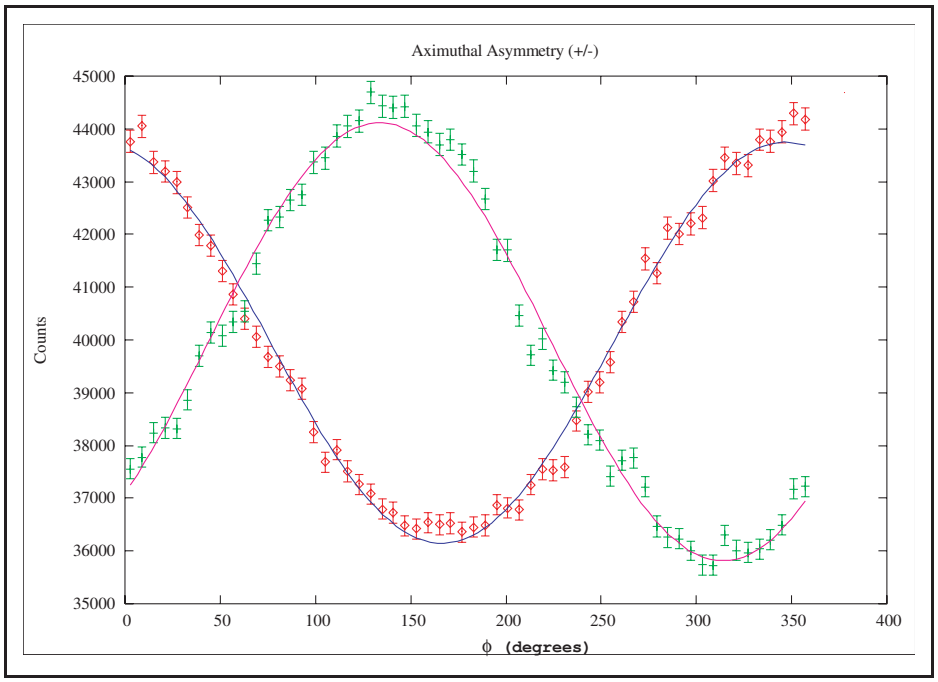

- Difference between 2 helicity states
  - instrumental asymmetries cancel, P_B and A_y cancel.
  - gain access to the polarization components

G_E^p in Hall A

Difference between 2 helicity states ($Q^2 = 5.6$)

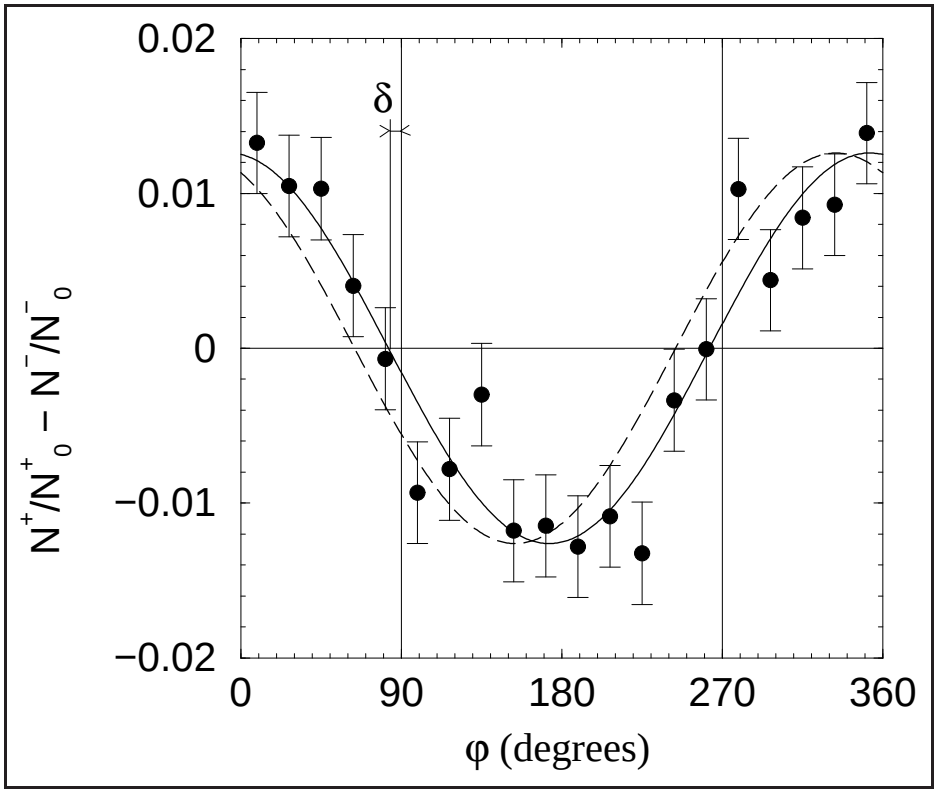

- Fit $N^+ - N^-$ with $F(\varphi) = C\cos(\varphi + \delta) \rightarrow \tan\delta = P_t^{\rm fpp}/P_n^{\rm fpp} \simeq 7^\circ$
- $P_n^{\rm fpp} = \sin\chi \cdot hP_l, \qquad P_t^{\rm fpp} = hP_t$
- $\frac{G_E}{G_M} = -\frac{P_t}{P_l}\frac{(E_e+E_{e'})}{2M_N}\tan(\frac{\theta_e}{2})$

G_E^p in Hall A – Results

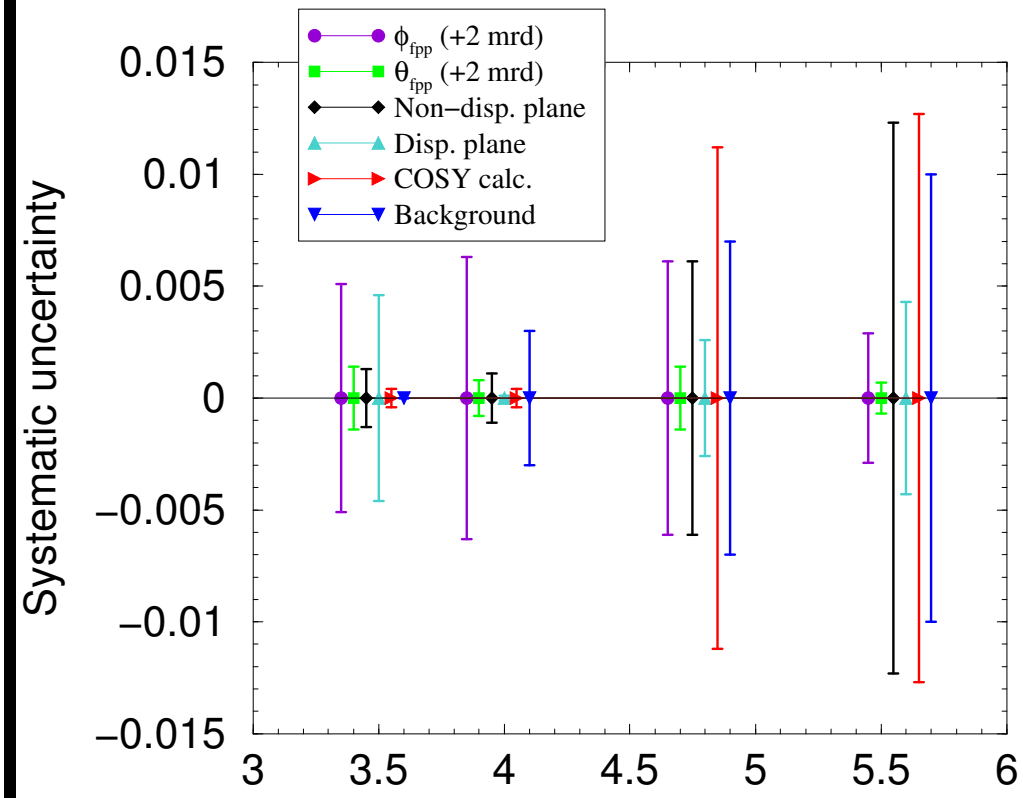

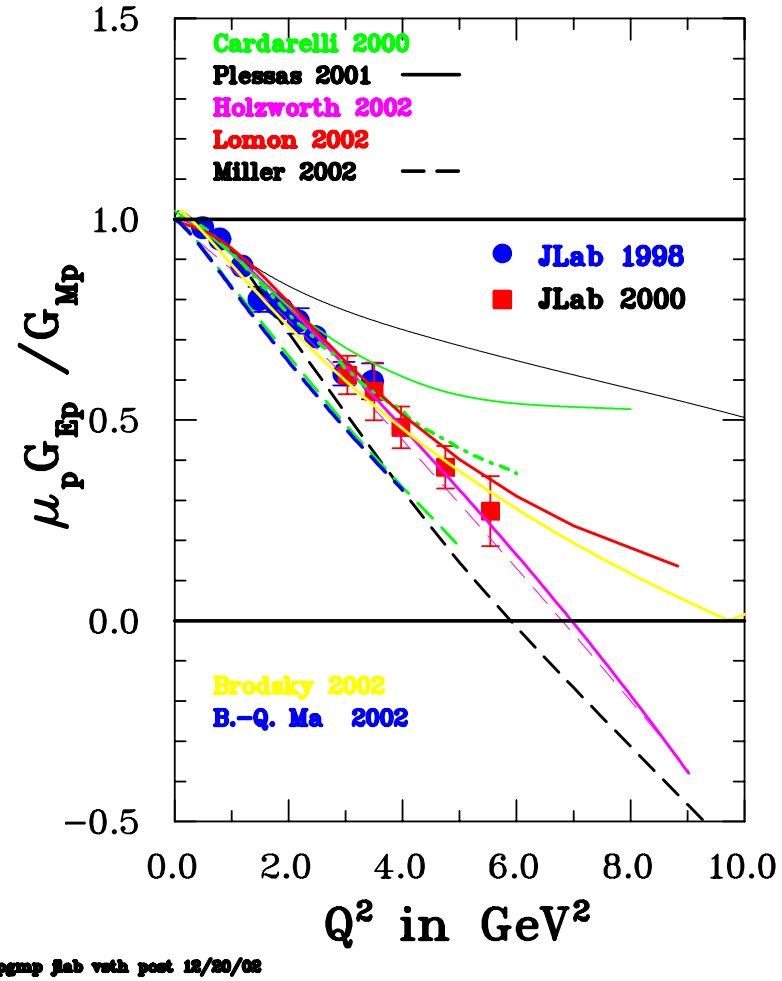

gepgmp jlab vath post 12/20/02

G_E^p in Hall A – Results

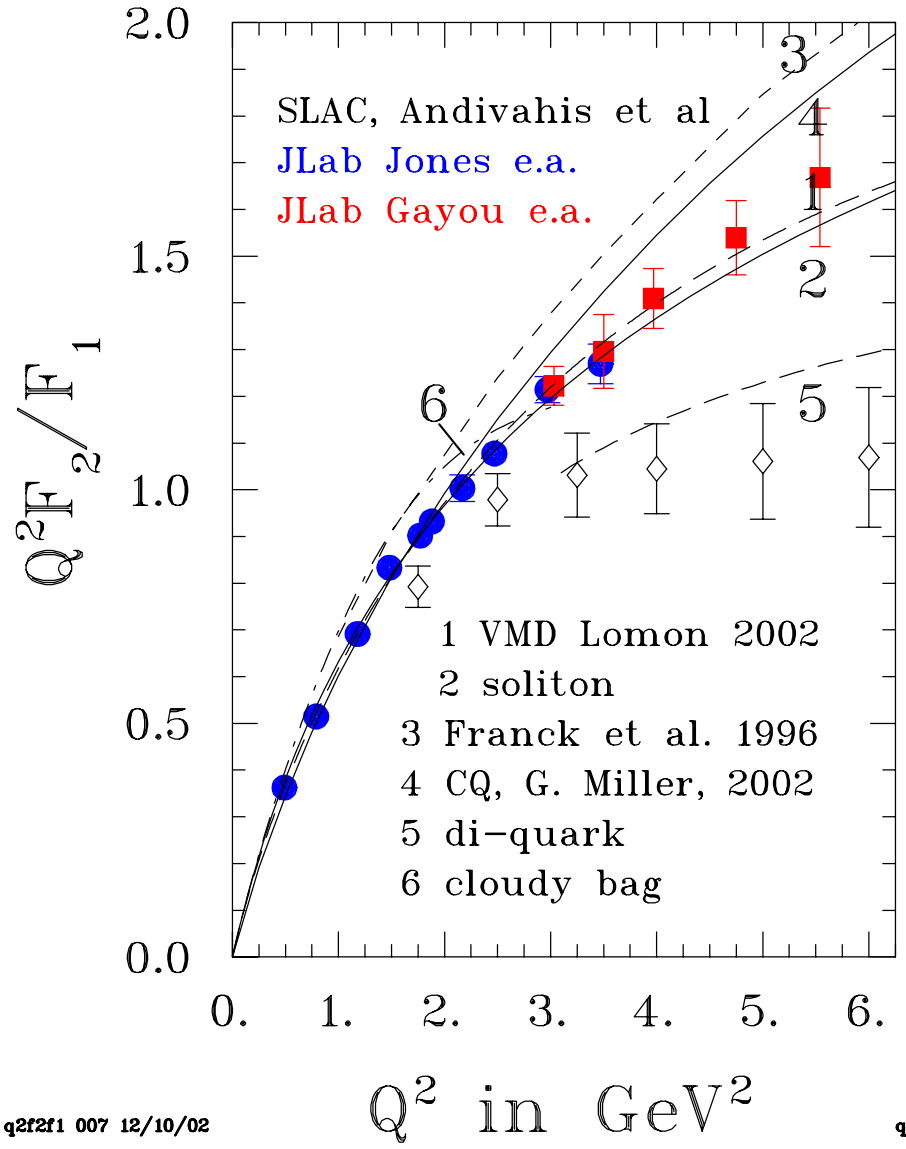

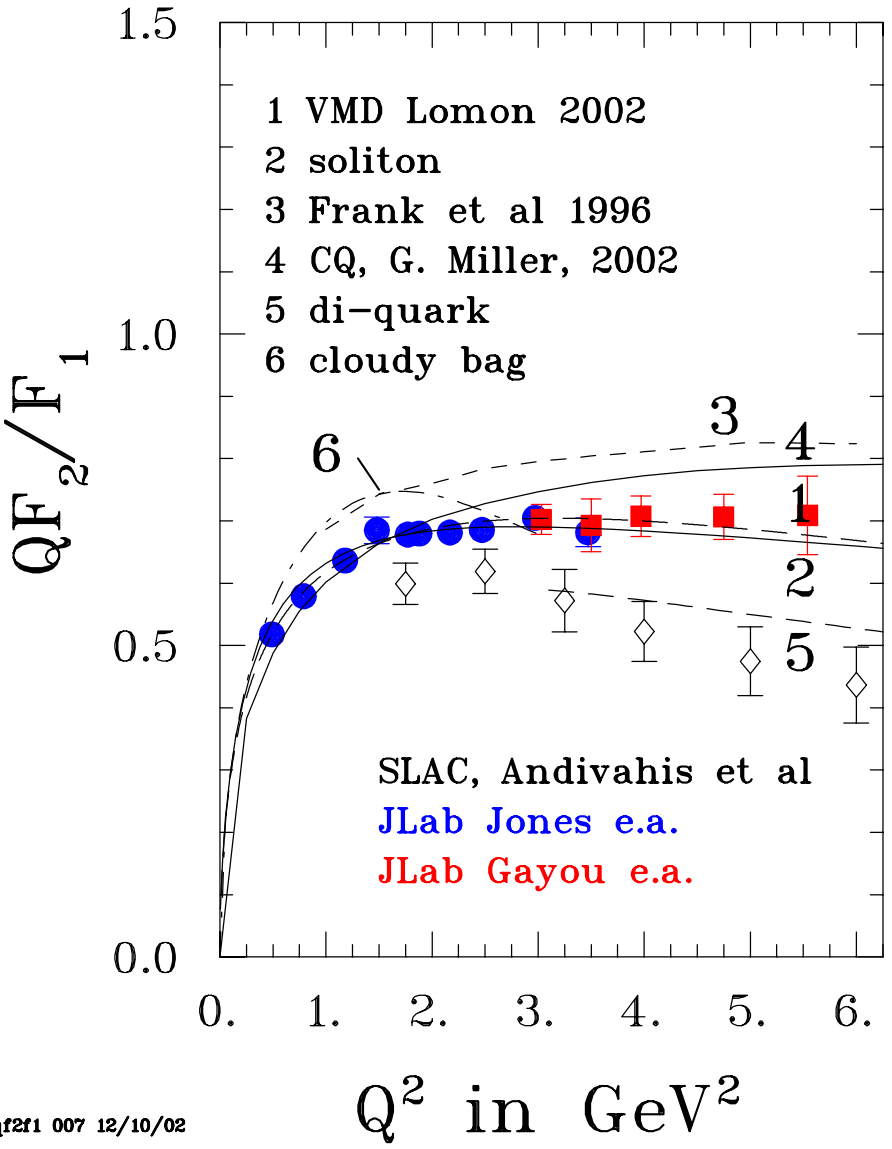

Interpretation

Considerable Attention - The two experiments have generated 250 citations.

Popular press - New York Times, USA Today, Science News...

What is the Shape of the Proton? G. Miller, RCQM

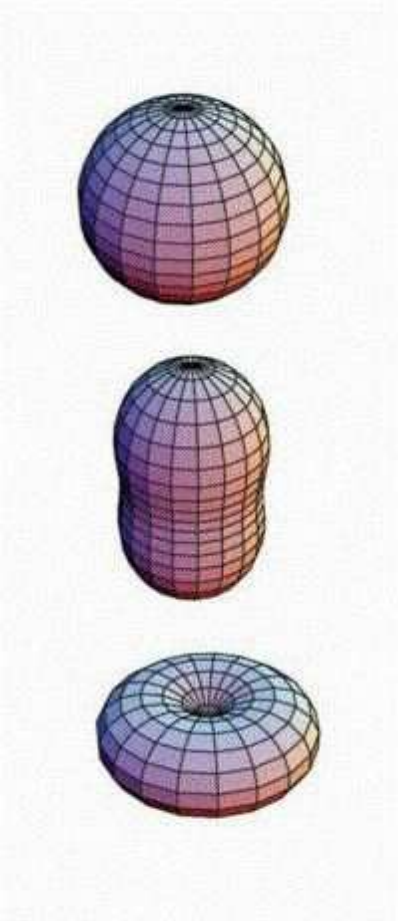

Momentum space representation, "normal" proton

High momentum quarks with spin aligned with proton

High momentum quarks with spin opposite to proton

G_E^n through recoil polarization

Recoil polarization, $^2\mathrm{H}(\vec{e}, e'\vec{n})p$, Mainz & JLAB

- ✷ In quasifree kinematics, $P_{s'}$ is sensitive to G_E^n and insensitive to nuclear physics
- ✷ Up–down asymmetry $\xi \Rightarrow$ transverse (sideways) polarization $P_{s'} = \xi_{s'}/P_e A_{\mathrm{pol}}$. Requires knowledge of P_e and A_{pol}
- ✷ Rotate the polarization vector in the scattering plane (with dipole magnet) and measure the longitudinal polarization, $P_{l'} = \xi_{l'}/P_e A_{\mathrm{pol}}$
- ✷ Take ratio, $\frac{P_{s'}}{P_{l'}}$. P_e and A_{pol} cancel
- ✷ E93038 at JLAB's Hall C: Three momentum transfers, $Q^2 = 0.45, 1.13,$ and $1.45(\mathrm{GeV/c})^2$.
- ✷ Data taking 2000/2001.

Notes on Extraction of the neutron form factors

No free neutron targets – scattering from a nucleus, D, ^{3}He

Neutron is not free - can not avoid engaging the details of the nuclear physics.

Minimize sensitivity to the how the reaction is treated and maximize the sensitivity to the neutron form factors by working in quasifree kinematics.

- ✷ Indirect measurements: The experimental asymmetries ($\xi_{s'}$, A_V^{ed}, $A_{\rm exp}^{qe}$) are compared to theoretical calculations.
- ✷ Theoretical calculations are generated for scaled values of the form factor.
- ✷ Form factor is extracted by comparison of the experimental asymmetry to acceptance averaged theory.

G_E^n in Hall C via $^2\mathrm{H}(\vec{e}, e'\vec{n})p$

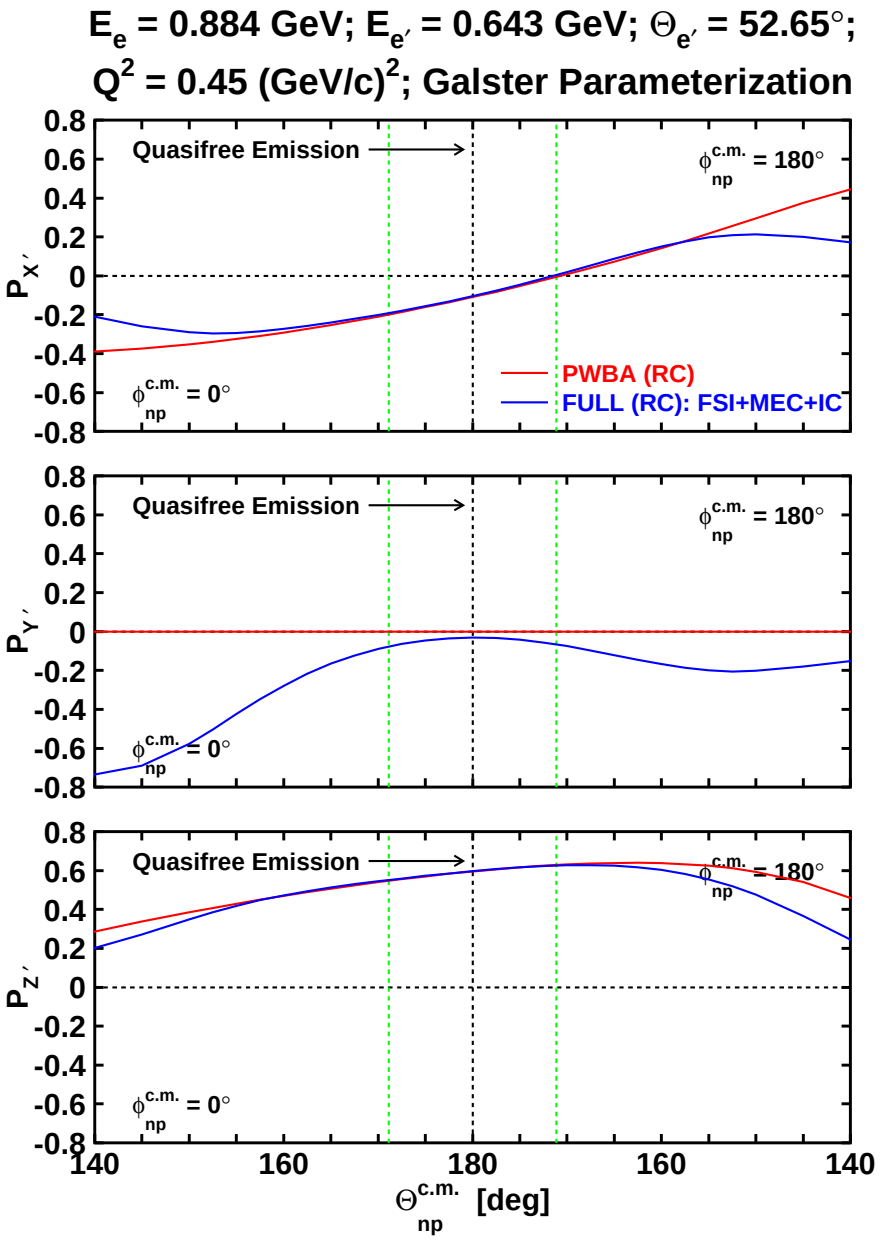

G_E^n in Hall C via $^2\mathrm{H}(\vec{e}, e'\vec{n})p$

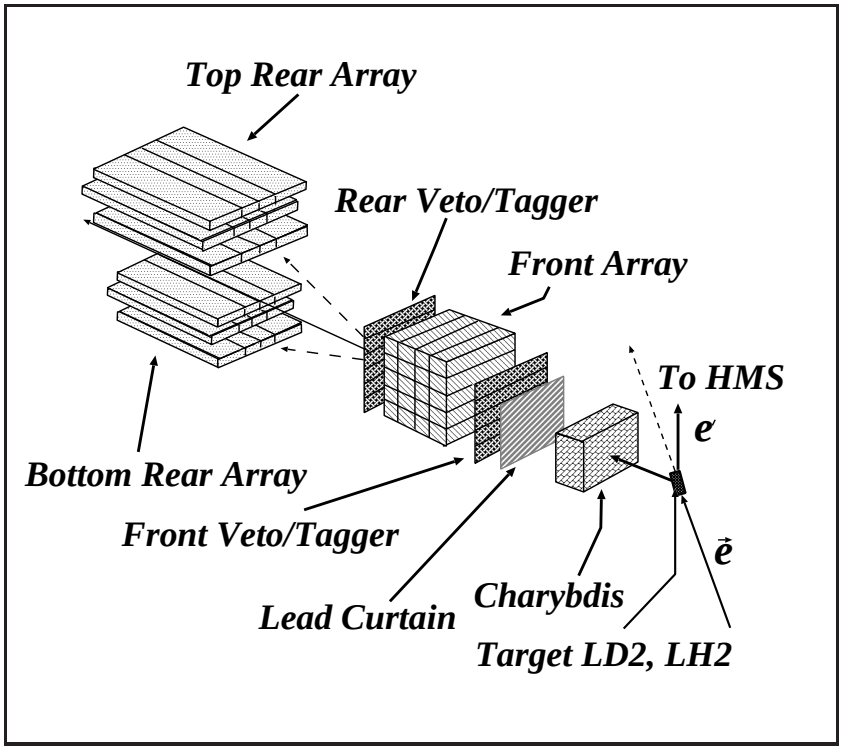

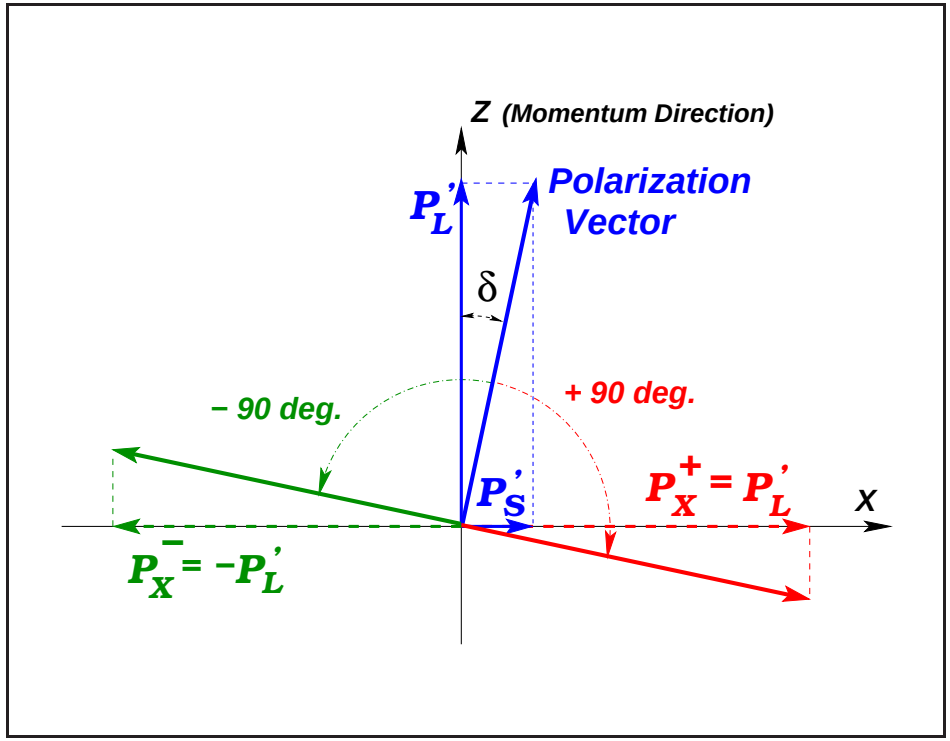

Taking the ratio eliminates the dependence on the analyzing power and the beam polarization → greatly reduced systematics

$$\frac{G_E^n}{G_M^n} = K \tan\delta \qquad \text{where} \qquad \tan\delta = \frac{P_{s'}}{P_{l'}} = \frac{\xi_{s'}}{\xi_{l'}}$$

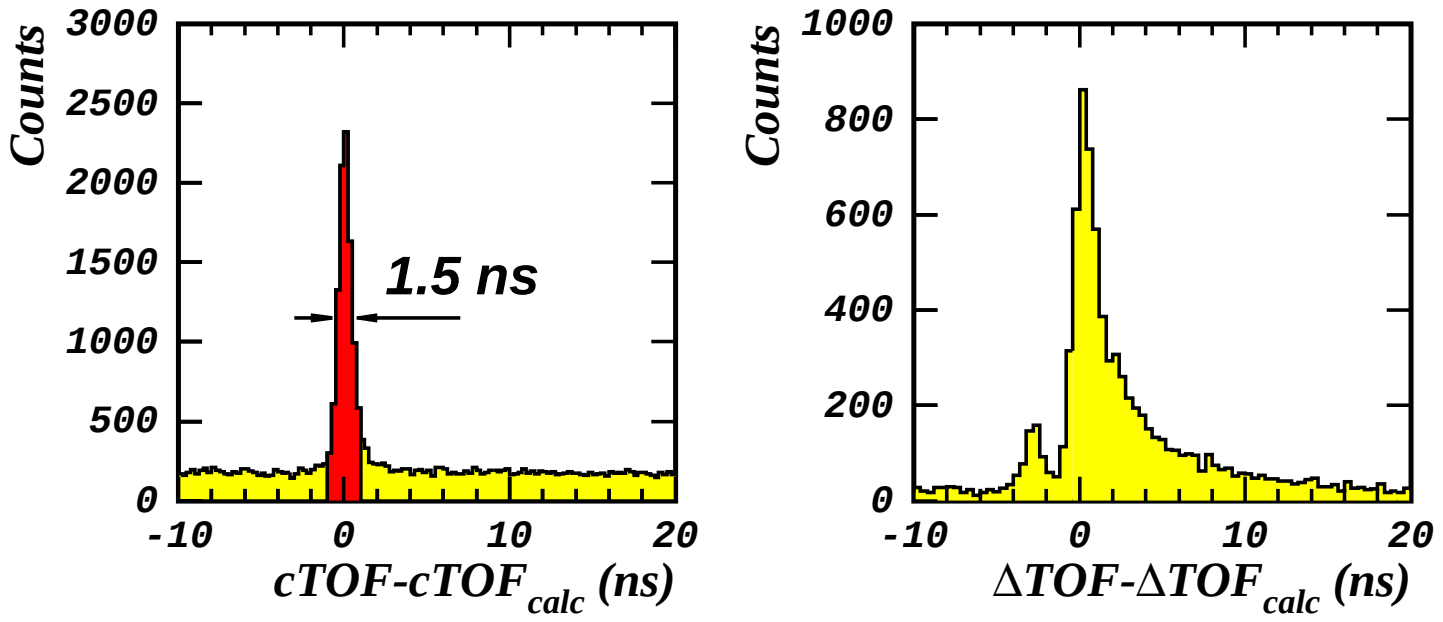

Left: Coincidence TOF for neutrons. Difference between measured TOF and calculated TOF assuming quasi-elastic neutron. Right: ΔTOF for neutron in front array and neutron in rear array.

ΔTOF is kept as the four combinations of (-,+) helicity, and (Upper,Lower) detector and cross ratios formed. False asymmetries cancel.

$$r = \left(\frac{N_U^+ N_D^-}{N_U^- N_D^+} \right)^{1/2} \qquad \xi = (r-1)/(r+1)$$

G_E^n in Hall C via $^2\mathrm{H}(\vec{e}, e'\vec{n})p$

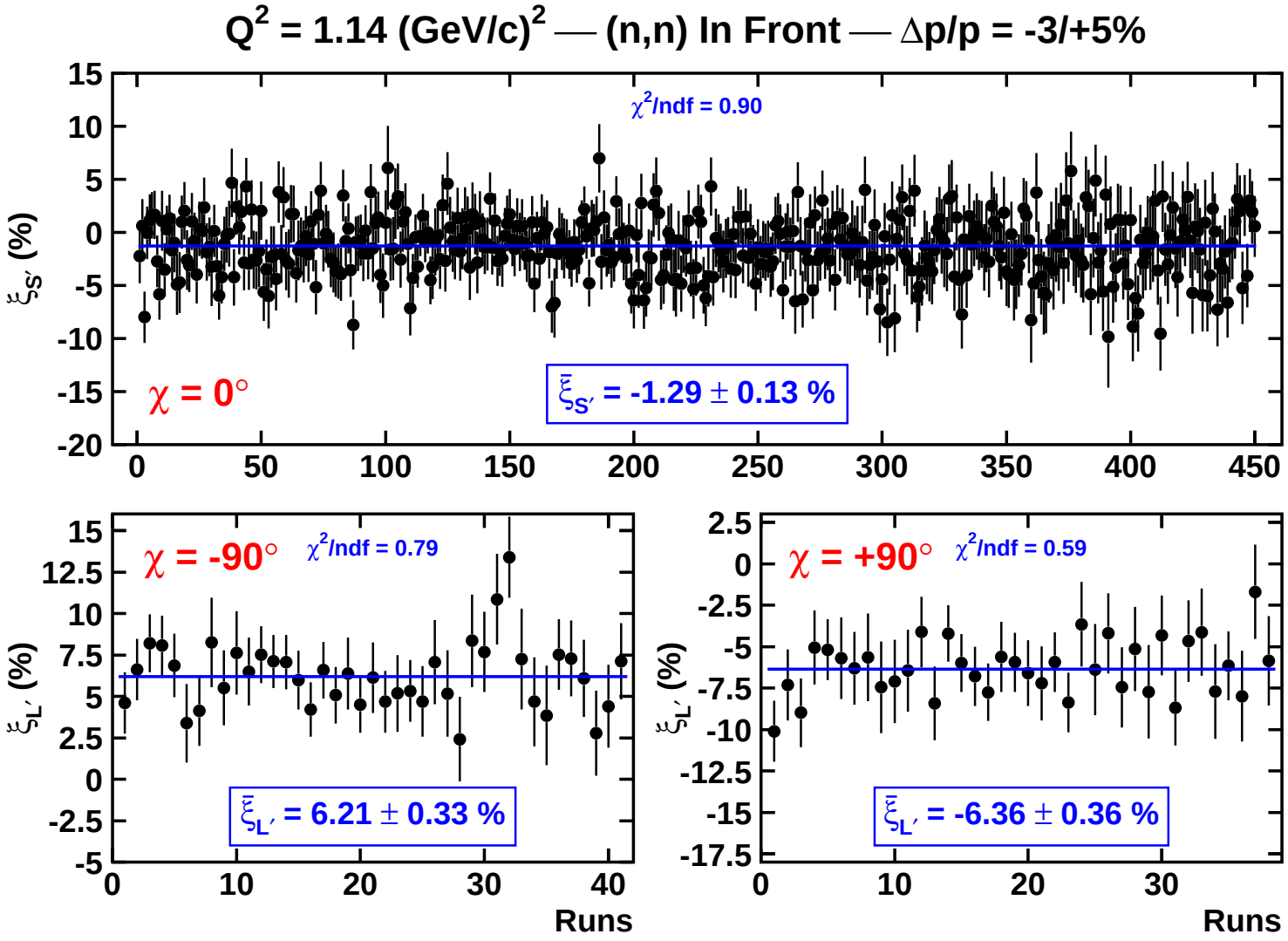

G_E^n in Hall C via $^2\mathrm{H}(\vec{e}, e'\vec{n})p$

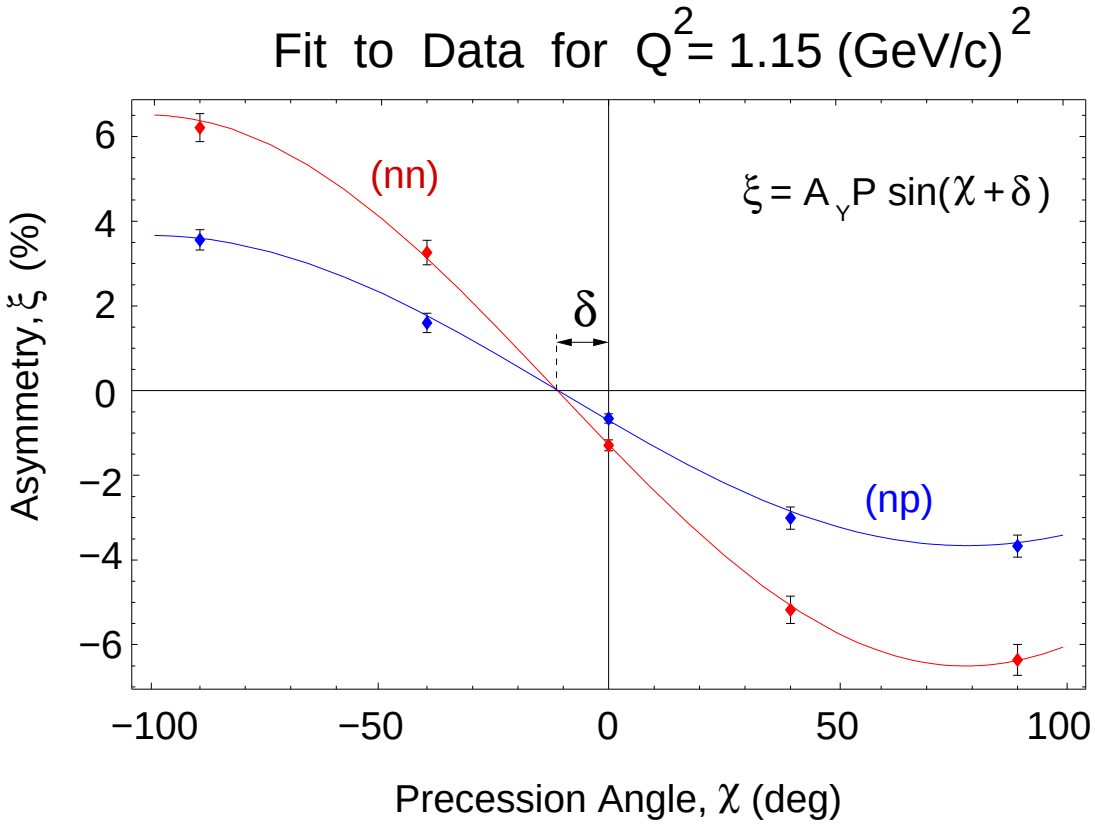

G_E^n via $^2\mathrm{H}(\vec{e}, e'\vec{n})p$

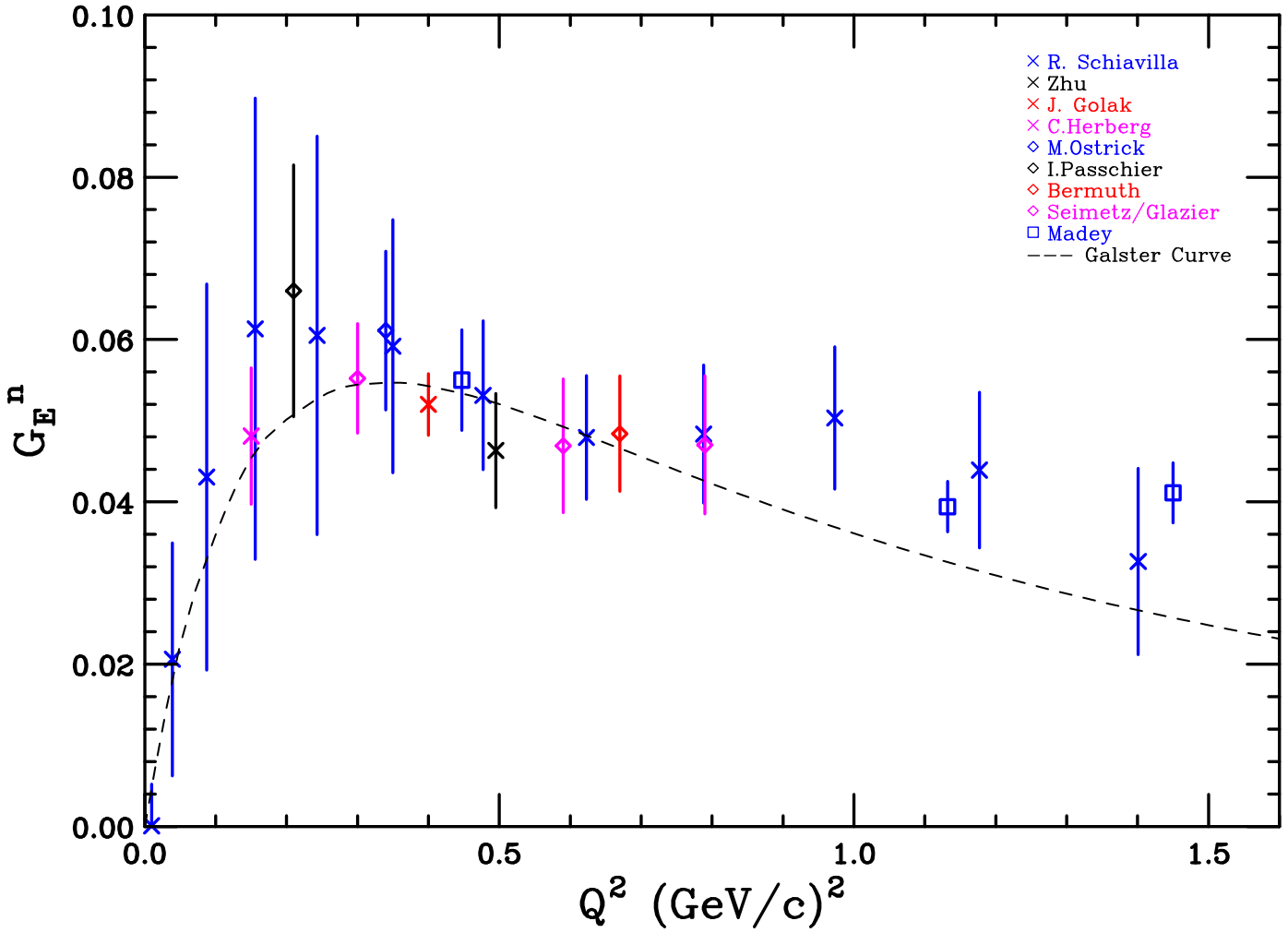

Beam–Target Asymmetry - Principle

Polarized Cross Section:

$\sigma = \Sigma + h\Delta$

Beam Helicity $h \pm 1$

$$A = \frac{\sigma_+ - \sigma_-}{\sigma_+ + \sigma_-} = \frac{\Delta}{\Sigma}$$

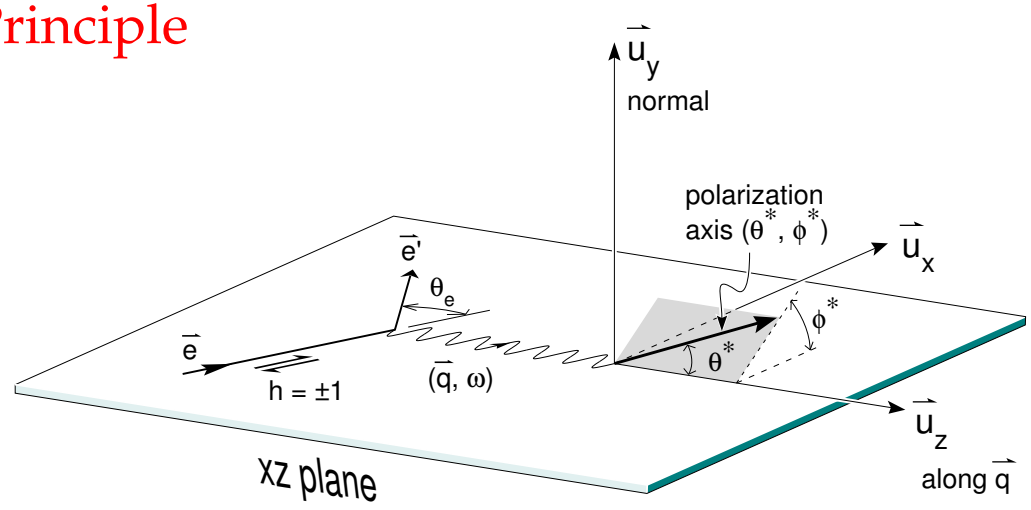

$$A = \frac{\overbrace{a\cos\Theta^\star (G_M)^2}^{A_T} + \overbrace{b\sin\Theta^\star\cos\Phi^\star G_E G_M}^{A_{TL}}}{c\,(G_M)^2 + d\,(G_E)^2}; \quad \varepsilon = \frac{N^\uparrow - N^\downarrow}{N^\uparrow + N^\downarrow} = P_B \cdot P_T \cdot f \cdot A$$

$\Theta^\star = 90^\circ \quad \Phi^\star = 0^\circ$

$$\Longrightarrow A = \frac{bG_E G_M}{c\,(G_M)^2 + d\,(G_E)^2}$$

$\Theta^\star = 0^\circ \quad \Phi^\star = 0^\circ$

$$\Longrightarrow A = \frac{aG_M^2}{c\,(G_M)^2 + d\,(G_E)^2}$$

Beam–Target Asymmetry - Practice

- No free neutron
- Unpolarized materials
- Protons dominate
- The deuteron and ^{3}He only approximate a polarized neutron
- Scattering from other polarized materials
- Indirect measurement of form factors
- Taking ratio of A_{TL}/A_T not always practical; errors arising from P_t and P_b

Beam–Target Asymmetry in E93-026

$^2\overrightarrow{\mathrm{H}}(\overrightarrow{e}, e'n)p$

$$\sigma(h,P) \approx \sigma_0 \left(1 + hPA_{ed}^V + hTA_{ed}^T\right)$$

h: Beam Helicity

P: Vector Target Polarization

T: Tensor Target Polarization $T = 2 - \sqrt{4 - 3P^2}$

A_d^T is suppressed by $T \approx 3\%$

Theoretical Calculations of electrodisintegration of the deuteron by H. Arenhövel and co-workers

E93-026 $\quad \overrightarrow{\mathrm{D}}(\overrightarrow{e}, e'n)p \quad$ $\sigma(h,P) = \sigma_0 \left(1 + hP A_{ed}^V\right)$

A_{ed}^V is sensitive to G_E^n

has low sensitivity to potential models

has low sensitivity to subnuclear degrees of freedom (MEC, IC)

in quasielastic kinematics

Sensitivity to G_E^n – Insensitivity to Reaction

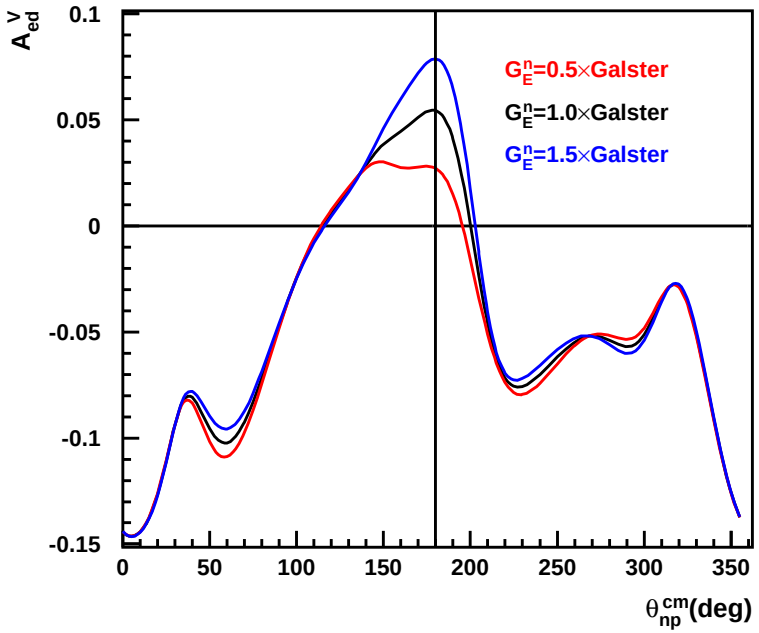

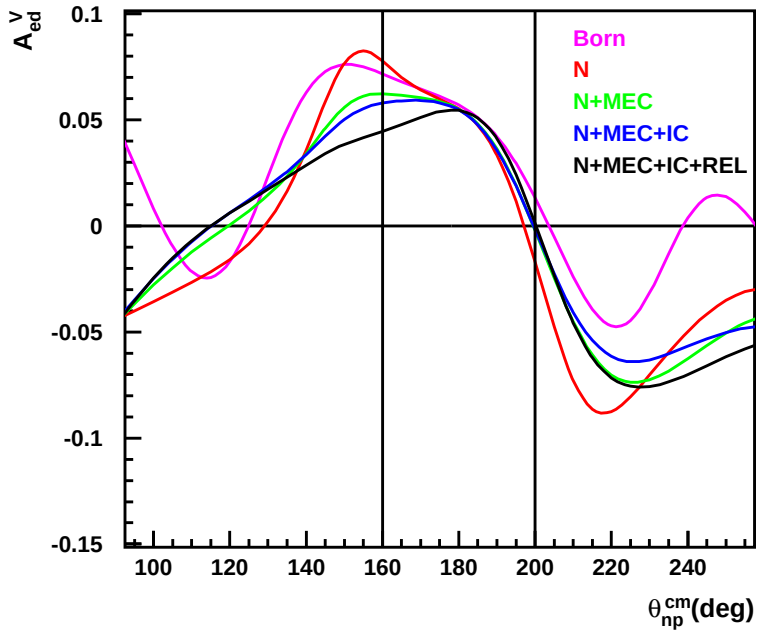

G_E^n in Hall C

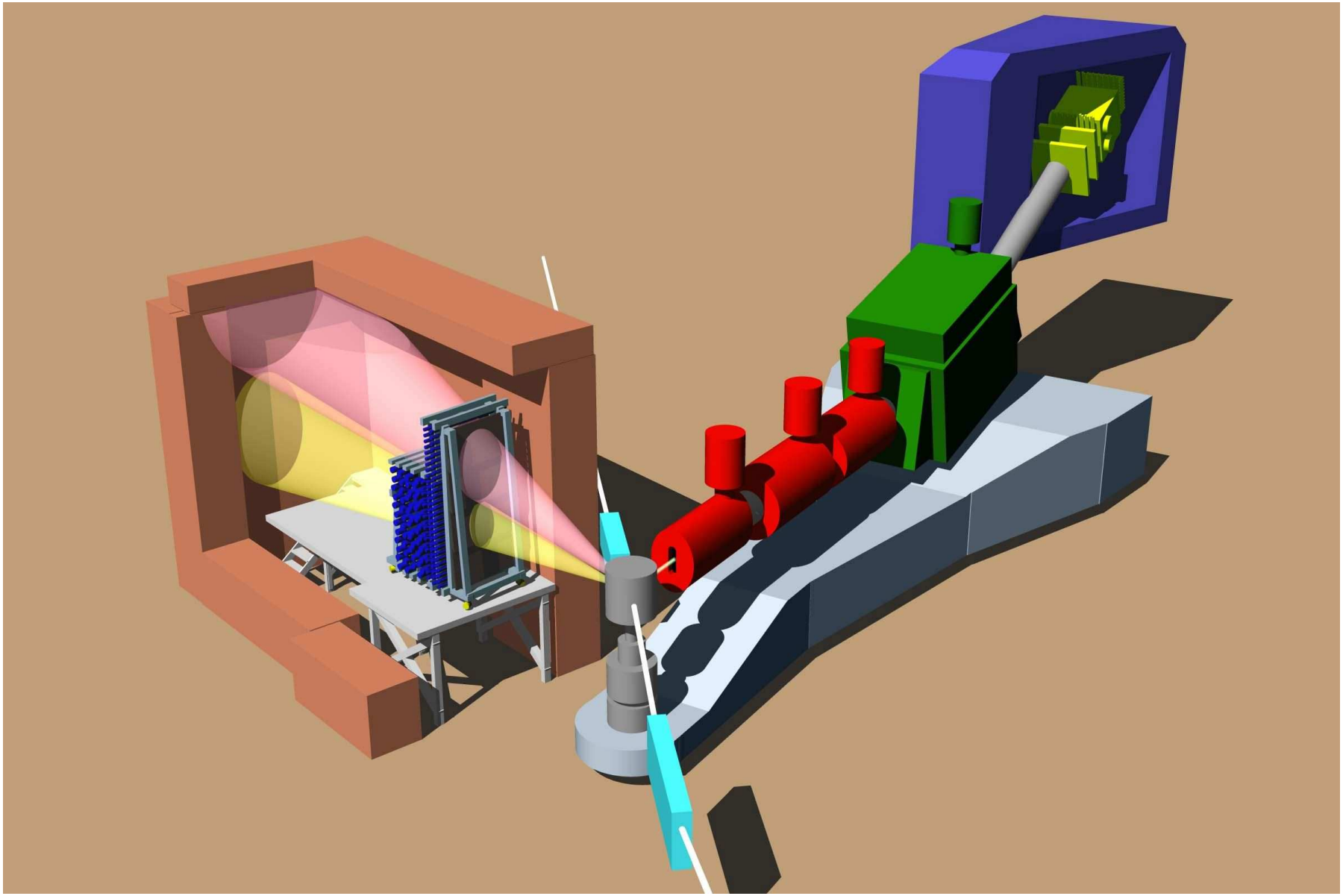

Notes on Hall C Setup

- Polarized Target
- Chicane to compensate for beam deflection of ≈ 4 degrees
- Scattering Plane Tilted
- Protons deflected ≈ 17 deg at $Q^2 = 0.5$
- Raster to distribute beam over 3 cm^2 face of target
- Electrons detected in HMS (right)
- Neutrons and Protons detected in scintillator array (left)
- Beam Polarization measured in coincidence Möller polarimeter

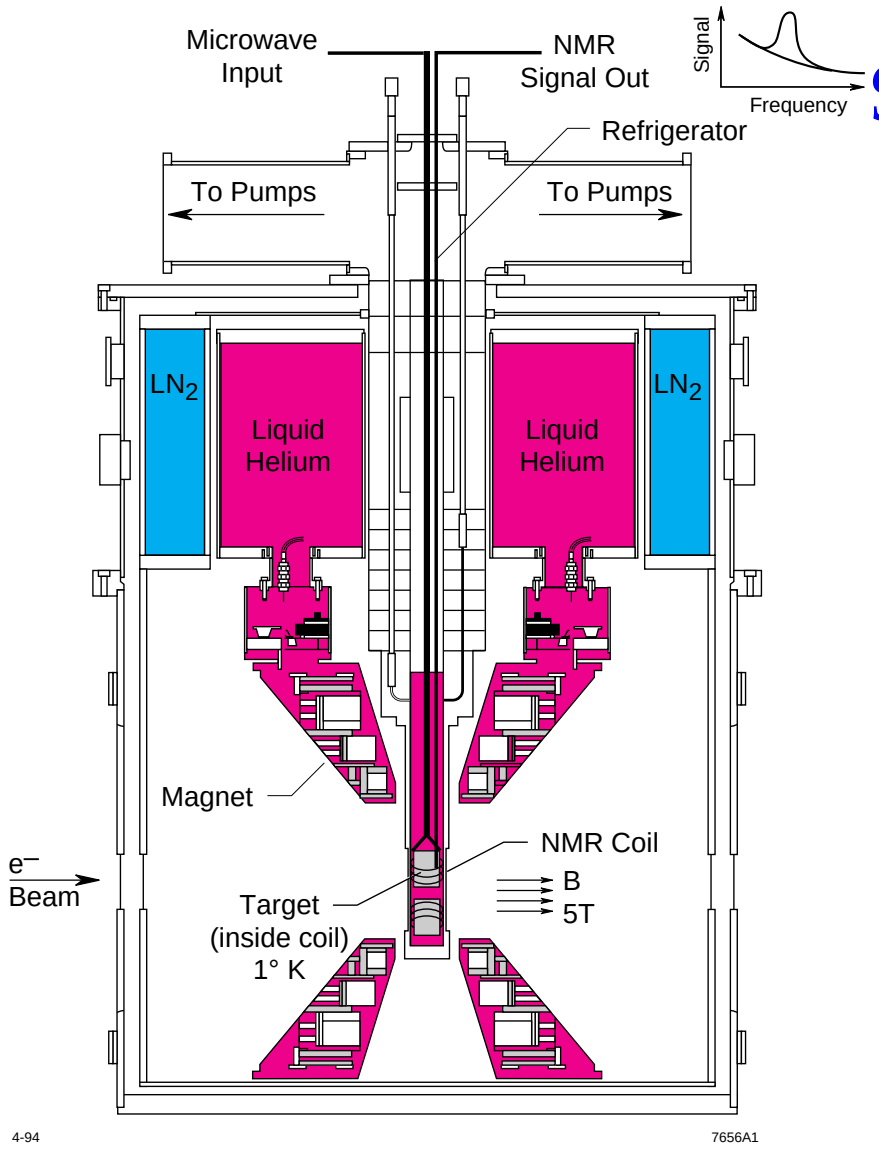

Solid Polarized Targets

- frozen(doped) $^{15}ND_3$
- ^{4}He evaporation refrigerator
- $5T$ polarizing field
- remotely movable insert
- dynamic nuclear polarization

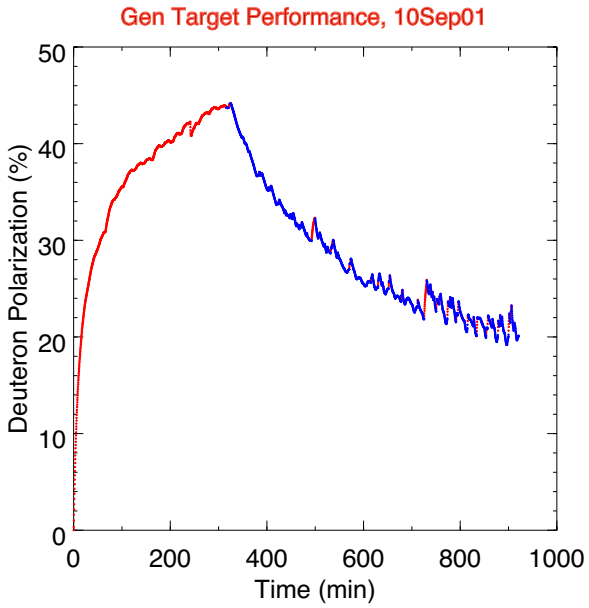

Neutron Detector

- Highly segmented scintillator
- Rates: 50 - 200 kHz per detector
- Pb shielding in front to reduce background
- 2 thin planes for particle ID (VETO)
- 6 thick conversion planes
- 142 elements total, >280 channels
- Extended front section for symmetric proton coverage
- PMTs on both ends of scintillator
- Spatial resolution $\simeq$ 10 cm
- Time resolution $\simeq$ 400 ps
- Provides 3 space coordinates, time and energy

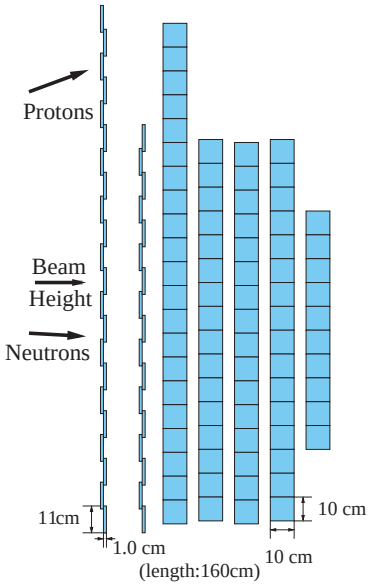

1998

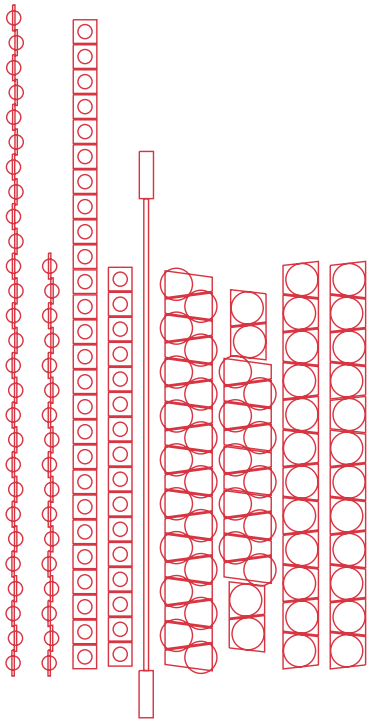

2001

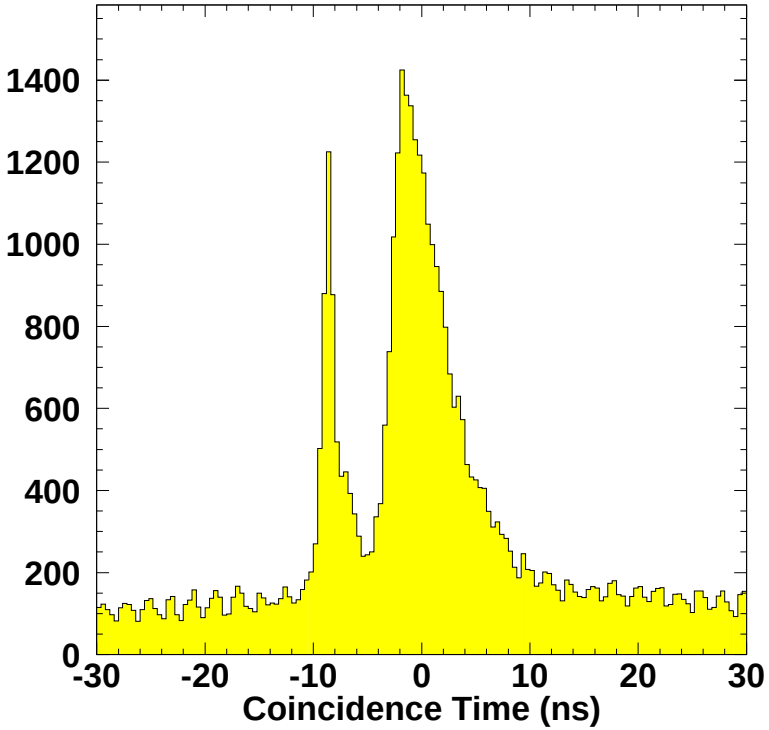

Experimental Technique for $\overrightarrow{\mathrm{D}}(\overrightarrow{e}, e'n)p$

For different orientations of h and P: $N^{hP} \propto \sigma\,(h, P)$

Beam-target Asymmetry:

$$\epsilon = \frac{N^{\uparrow\uparrow} - N^{\downarrow\uparrow} + N^{\downarrow\downarrow} - N^{\uparrow\downarrow}}{N^{\uparrow\uparrow} + N^{\downarrow\uparrow} + N^{\downarrow\downarrow} + N^{\uparrow\uparrow}} = hPfA_{ed}^{V}$$

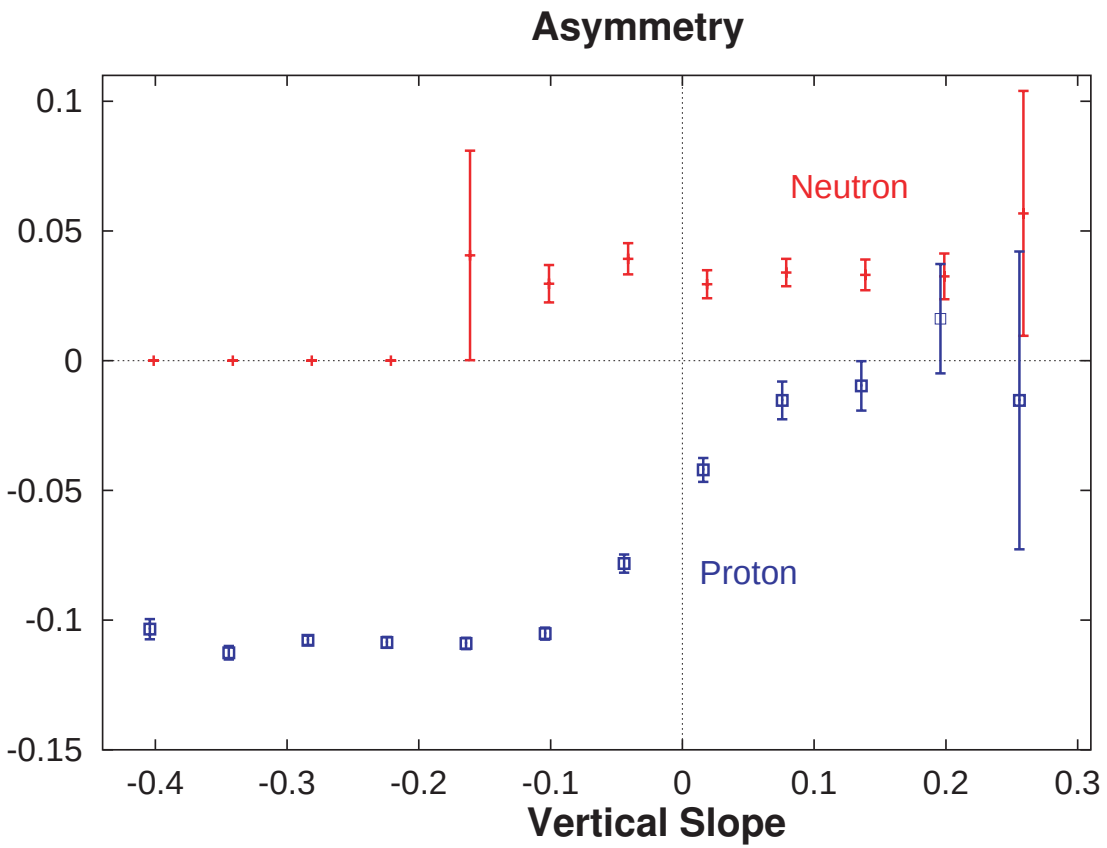

Data and MC Comparison

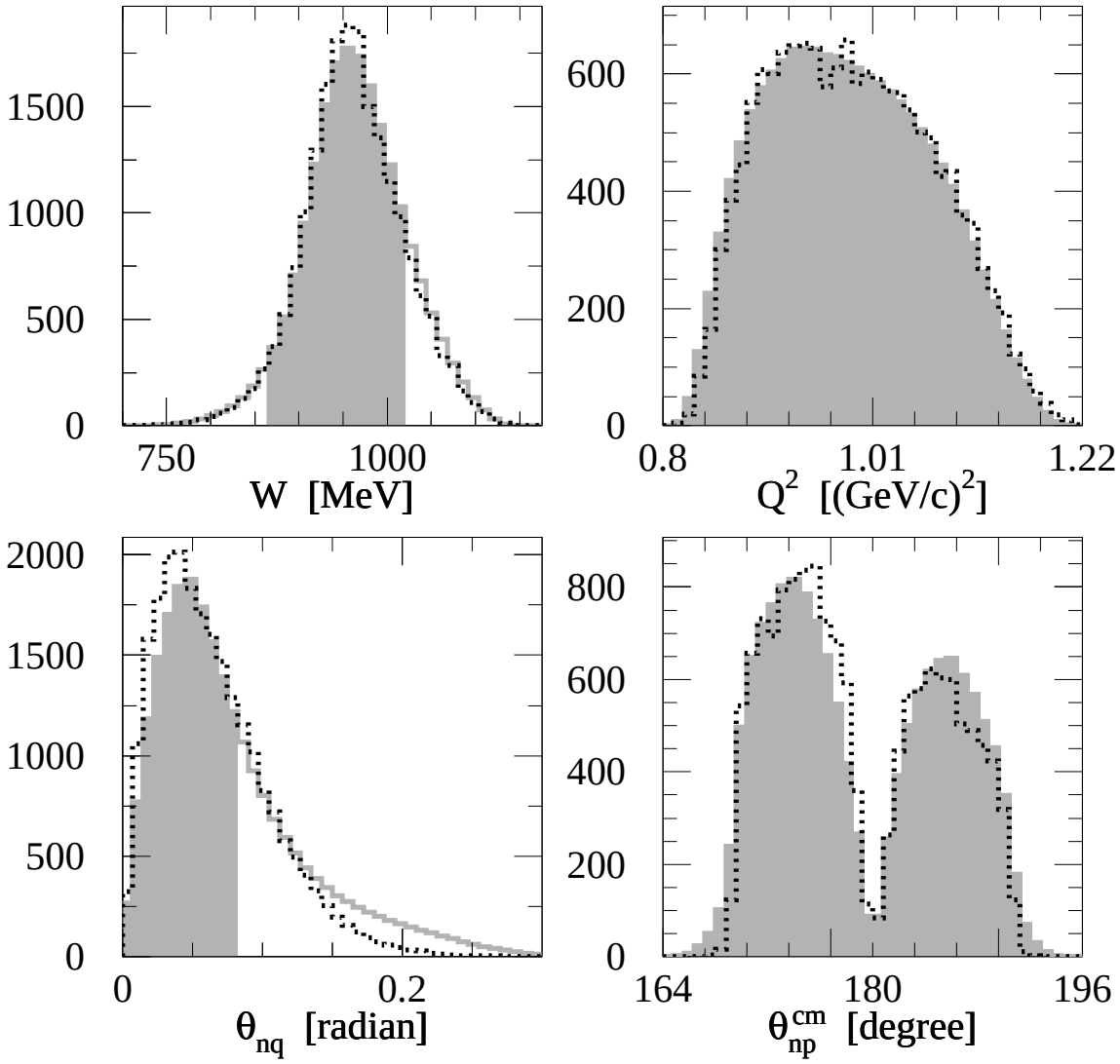

Extracting G_E^n

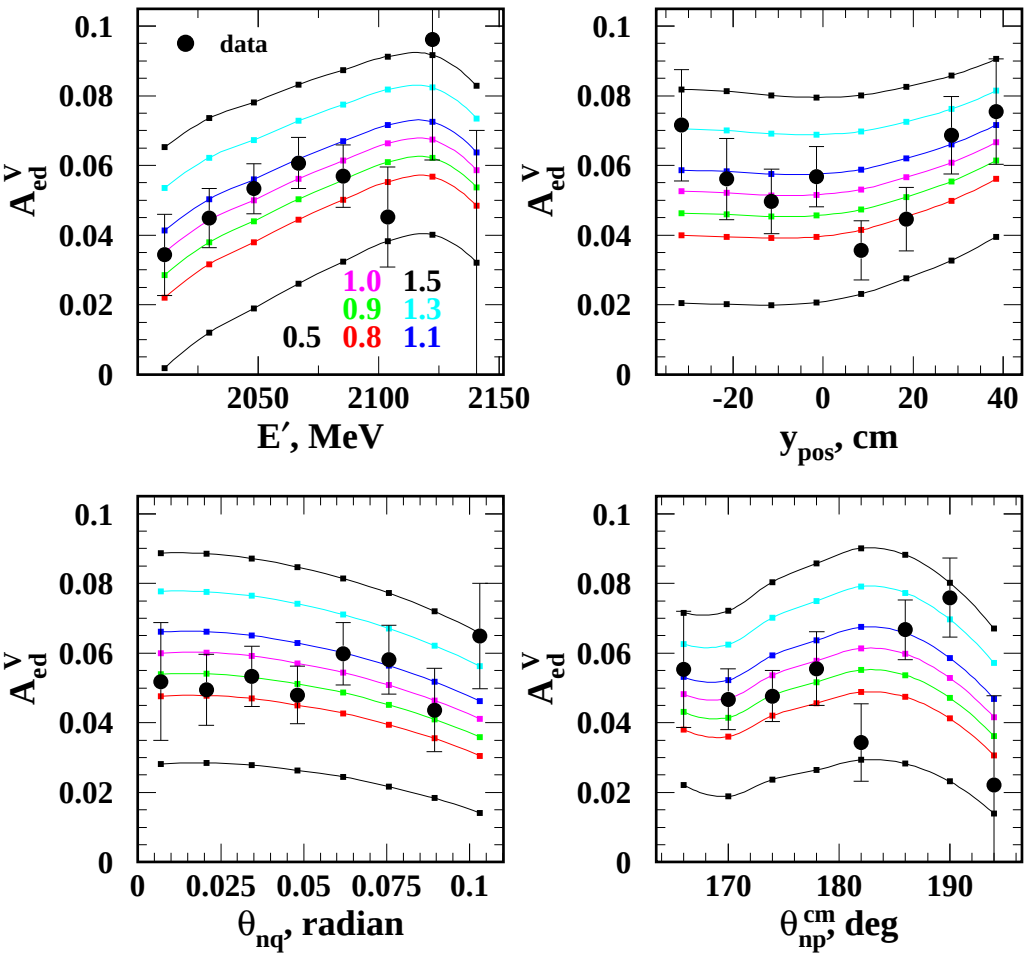

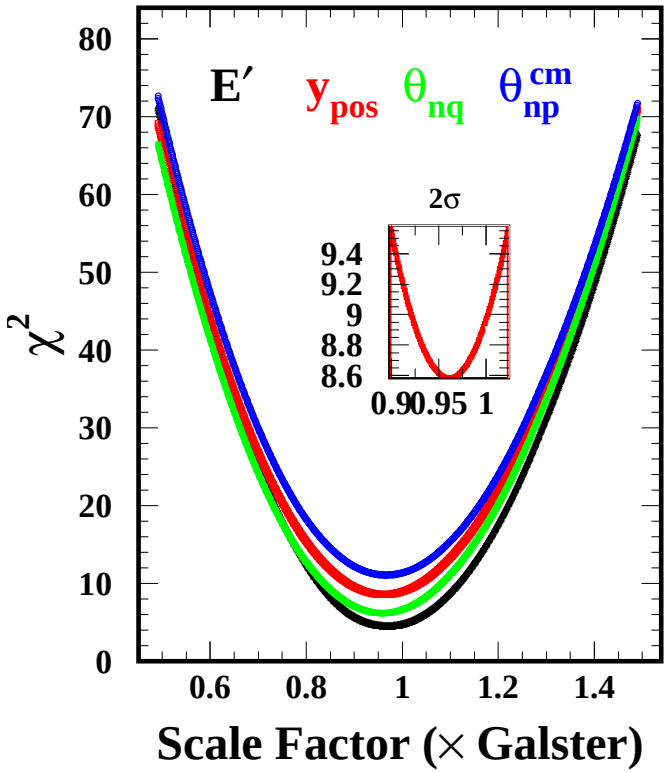

E93026 Results

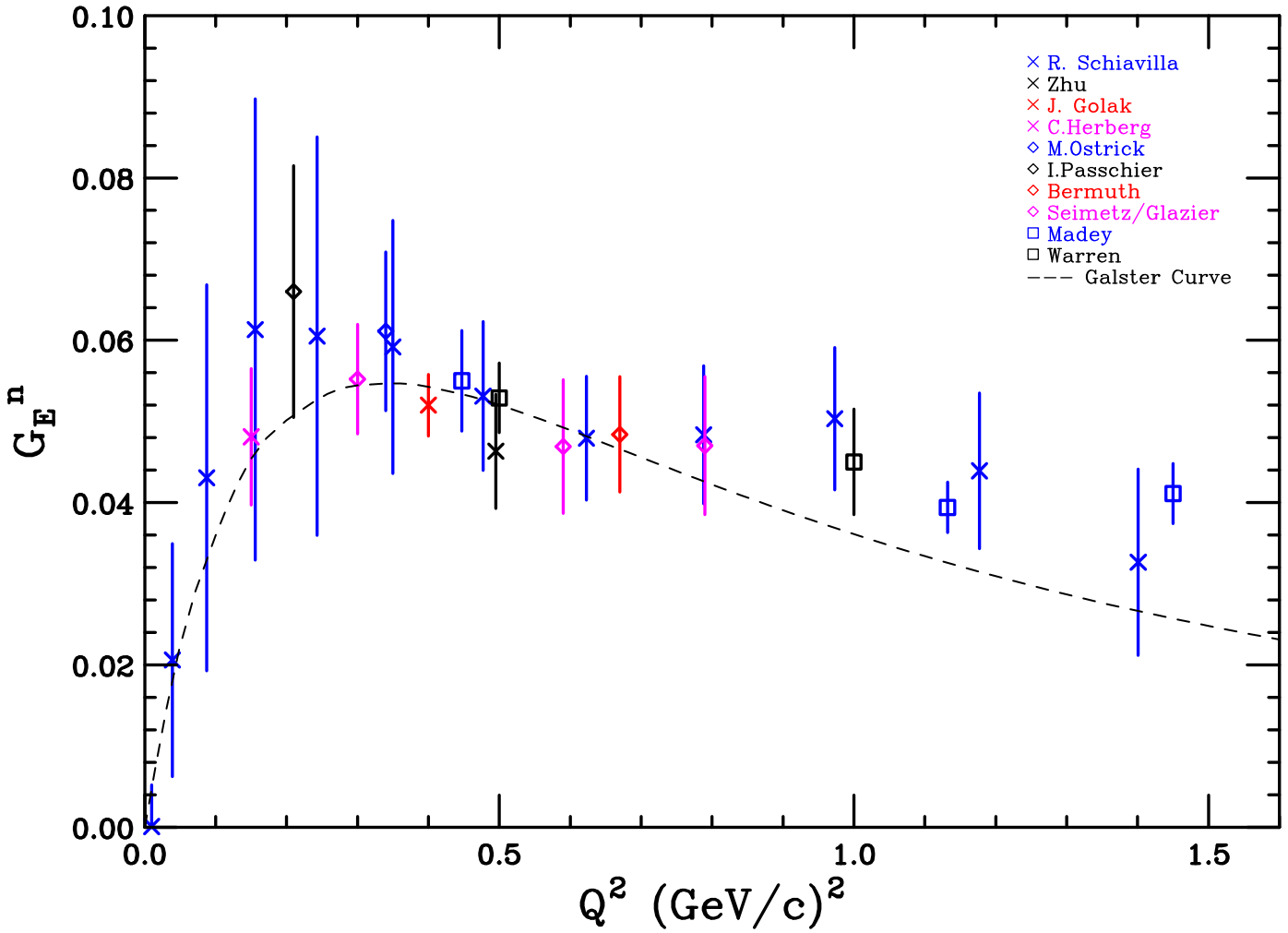

Relevant Theories

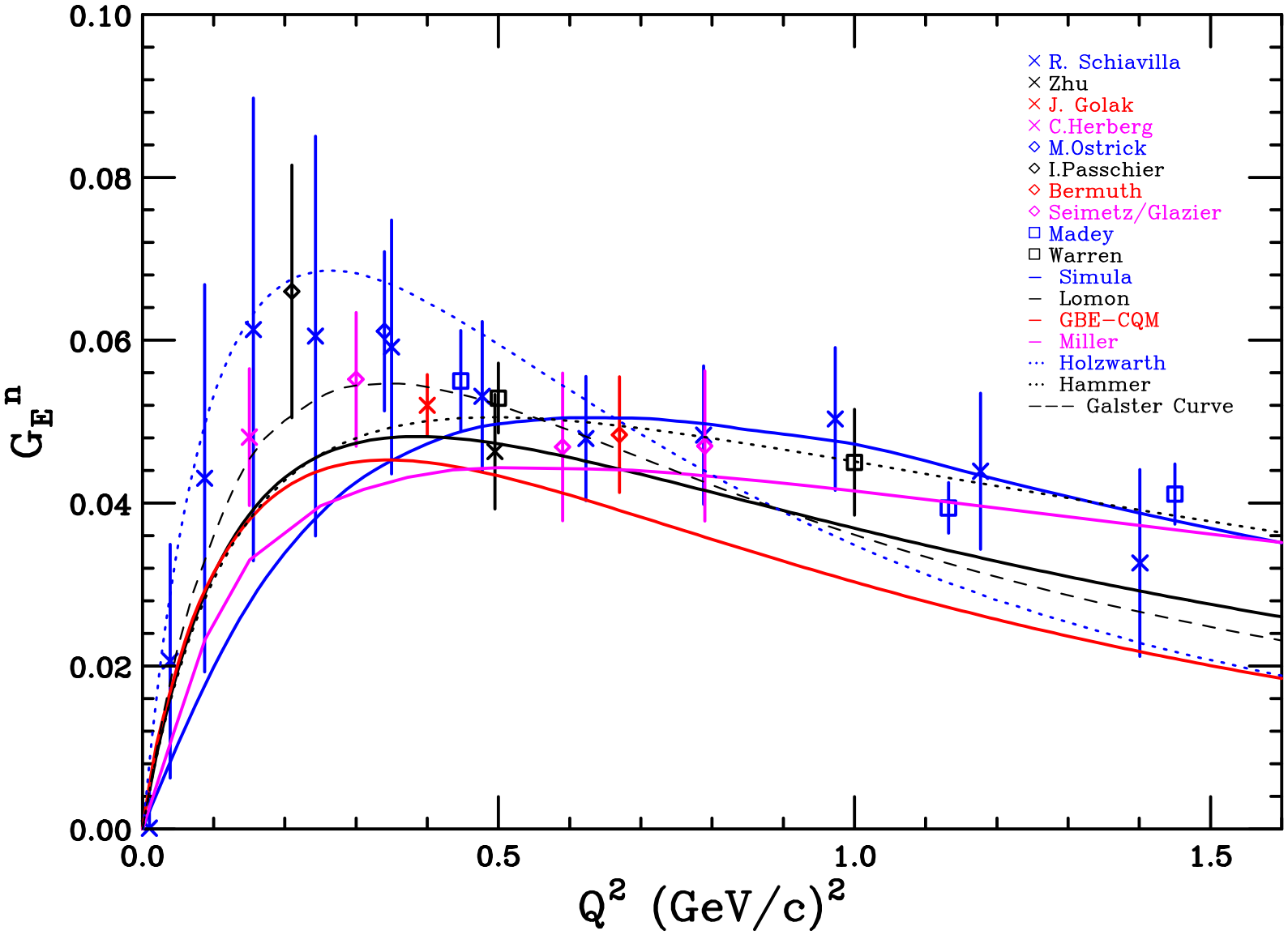

Systematic Errors

Systematic Errors (*included*):	
P_{target}	3-5%
f	3%
cuts	2%
kinematics	2%
G_M^n	1.7%
P_{beam}	1-3%
other	1%
total	**6-8%**

G_M^n via $\overrightarrow{^3\mathrm{He}}(\vec{e},e')X$, E95-001

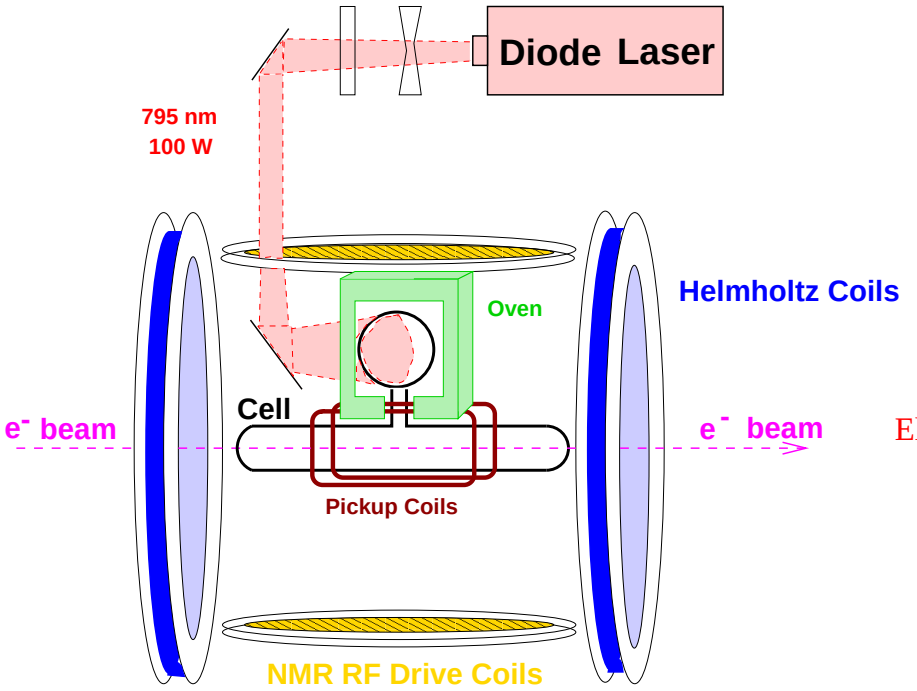

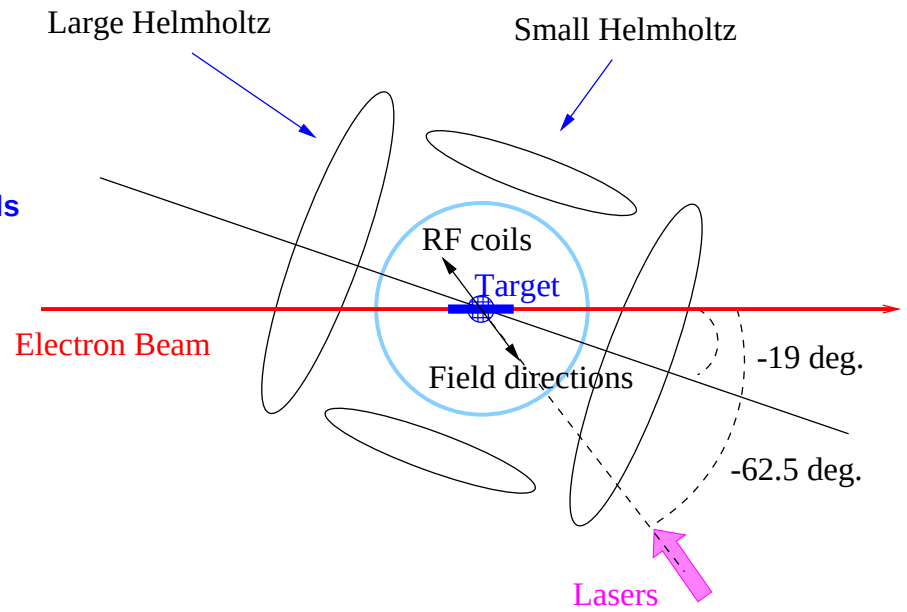

$$A_{\mathrm{raw}}^{\mathrm{qe}} = \frac{Y^{\mathrm{qe}}\uparrow - Y^{\mathrm{qe}}\downarrow}{Y^{\mathrm{qe}}\uparrow + Y^{\mathrm{qe}}\downarrow} = A_{\mathrm{exp}}^{\mathrm{qe}} \times P_b P_t$$

- Elastic scattering as monitor of $P_b P_t$. Very effective $\rightarrow 1.7\%$ contribution to error!
- P_t^+, P_t^-, h^+, h^- to minimize false asymmetries

G_M^n via $\overrightarrow{^3\mathrm{He}}(e,e')X$

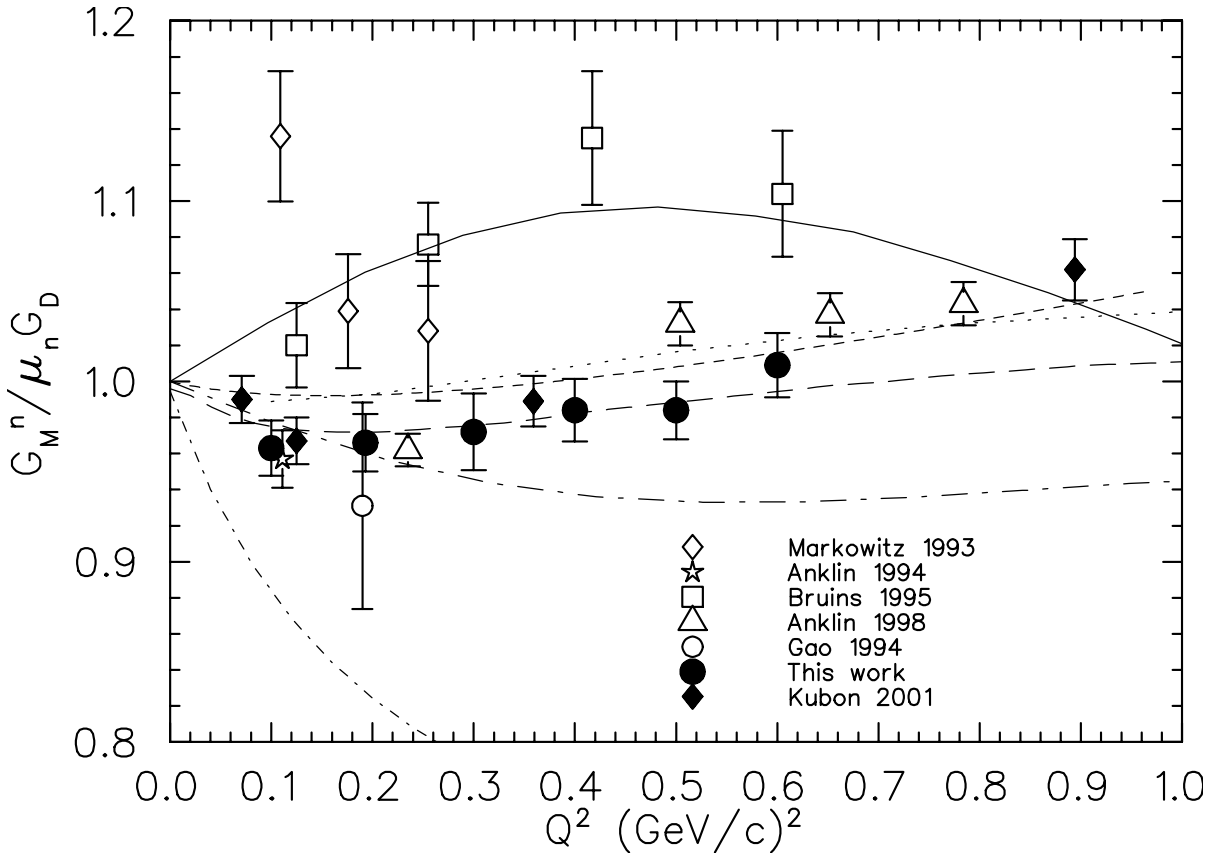

E95001, Wu *et al.*. PRC 67 012201(R) (2003)

- dots: Lomon
- short-dash: Holzwarth
- solid: Lu
- long dash: Mergell

G_M^n at High Q^2 in CLAS

Measure ratio of quasielastic $e-n$ scattering to quasielastic $e-p$ scattering off deuterium

$$R_D = \frac{\frac{d\sigma}{d\Omega}{}^{D(e,e'n)p}_{QE}}{\frac{d\sigma}{d\Omega}{}^{D(e,e'p)n}_{QE}} \approx \frac{f(G_M^n, G_E^n)}{f(G_M^p, G_E^p)}$$

Using the known values of G_E^p , G_M^p , G_E^n , extract G_M^n .

Has advantages over traditional techniques, $D(e,e')$, $D(e,e'\bar{p})n$, $D(e,e'n)p$

- ✳ No Rosenbluth separation or subtraction of dominant proton
- ✳ Ratio insenstive to deuteron model
- ✳ MEC and FSI are small in quasielastic region - don't get amplified by subtractions

Large acceptance to veto events with extra charged particles

Experimental Advantages/Demands

- Insensitive to
  - Luminosity
  - Electron radiative processes
  - Reconstruction and trigger efficiency
- Requires
  - Precise determination of absolute neutron detection efficiency
  - Equivalent solid angles for neutron and proton

Neutron Detection Efficiency

- Data taken with hydrogen and deuterium target simultaneously

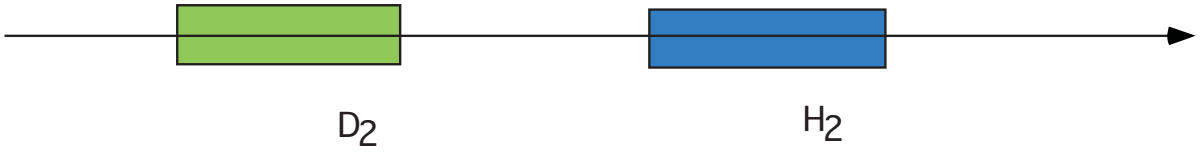

- tag neutrons with H_2 target via $H(e, e'n\pi^+)$
  - In-situ efficiency, timing, angular resolution determination
  - Insensitive to PMT gain variations
  - Small acceptance correction

CLAS ND efficiency

Insert CLAS-Gmn-ND-eff.pdf here

- Two beam energies, two field polarities
- G_M^n at the same Q^2 in different parts of drift chambers and magnetic field
- Neutrons detected in forward calorimeter, large angle calorimeter

Overlapping Measurements of G_n^M

(Semi-schematic)

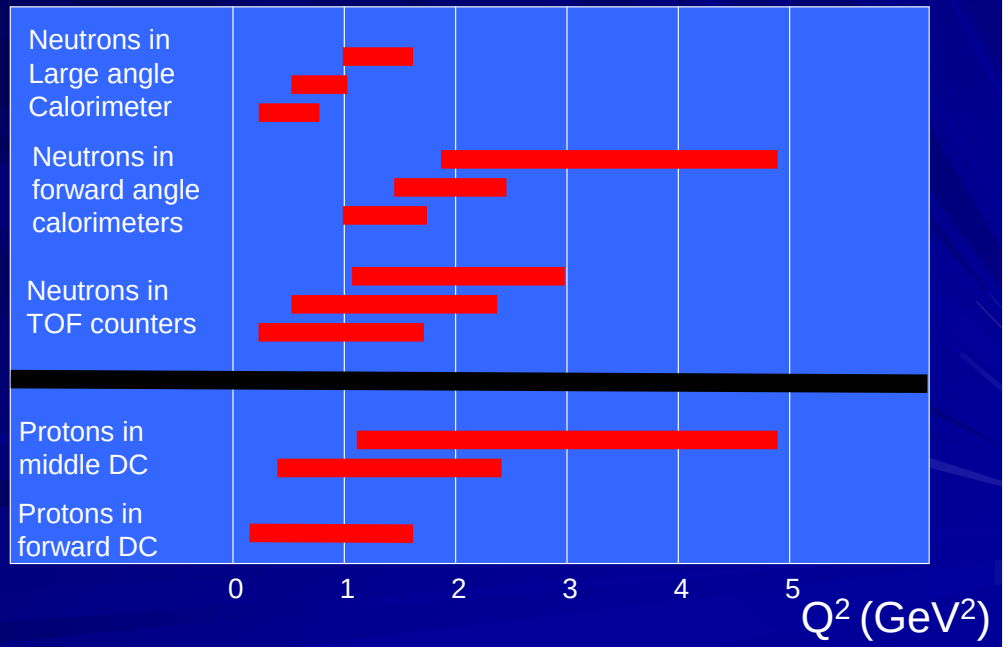

G_M^n Preliminary results from CLAS

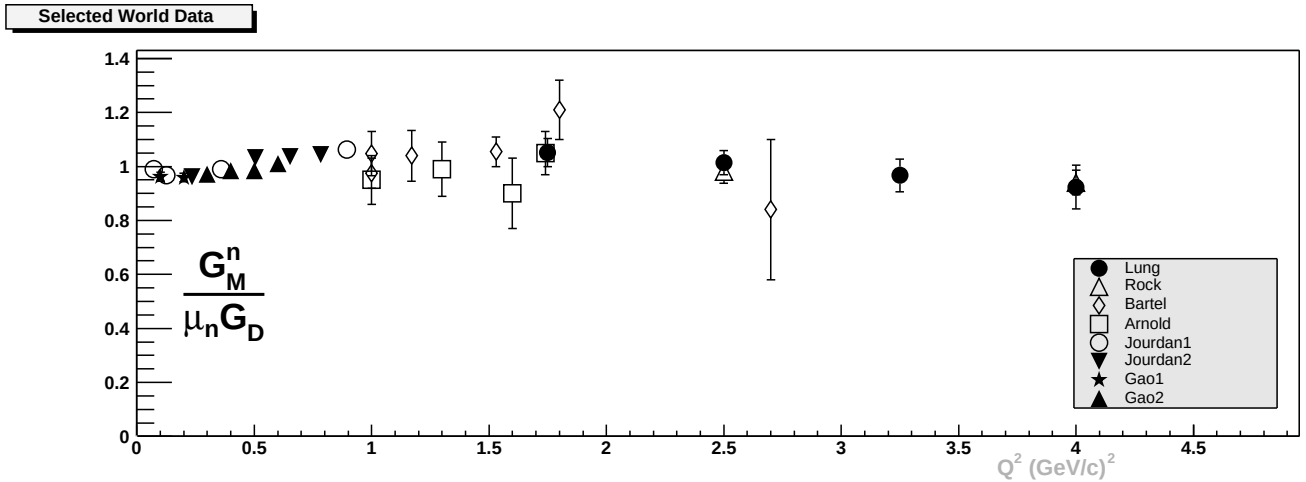

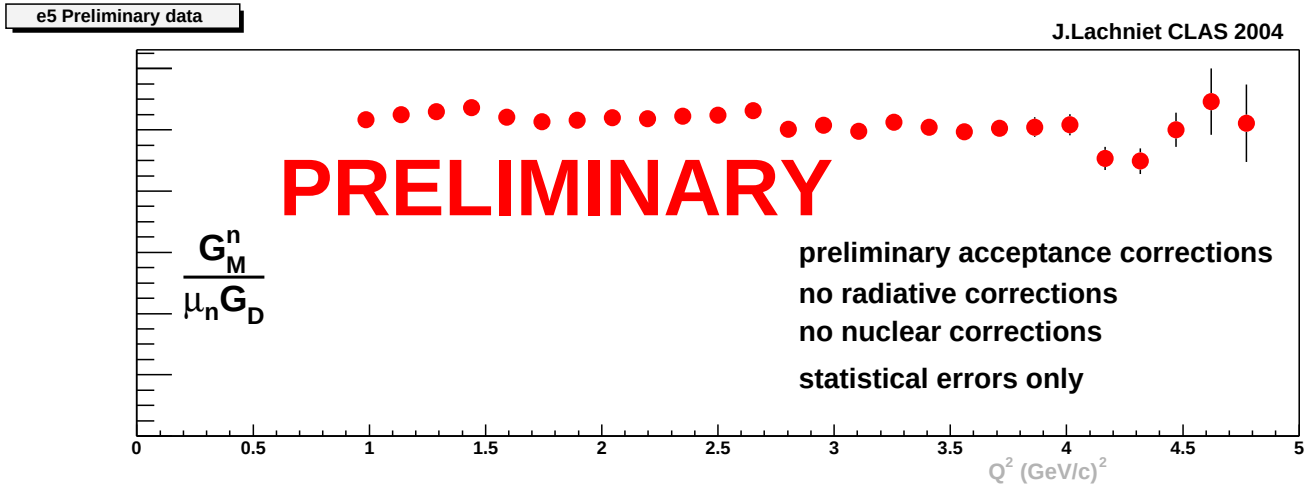

Preliminary results show a minimal deviation from dipole in contrast to the modern parametrization of the historical data set which shows a 10-15% deviation from the new Hall B data.

G_E^p , Status of Rosenbluth Separations

$$\sigma_R \equiv \frac{d\sigma}{d\Omega}\frac{\epsilon(1+\tau)}{\sigma_{Mott}} = \tau G_m^2(Q^2) + \epsilon G_E^2(Q^2)$$

Fundamental problem: σ insensitive to G_E^p at large Q^2. With $\mu G_E^p = G_M^p$, G_E^p contributes 8.3% to total cross section at $Q^2 = 5$.

$$\delta G_E \propto \delta(\sigma_R(\epsilon_1) - \sigma_R(\epsilon_2))(\Delta\epsilon)^{-1}(\tau G_M^2/G_E^2)$$

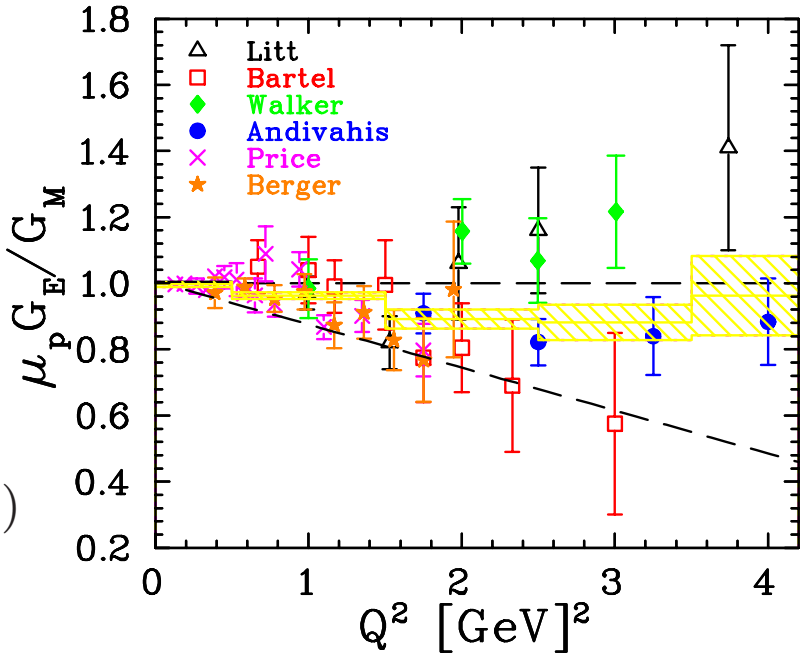

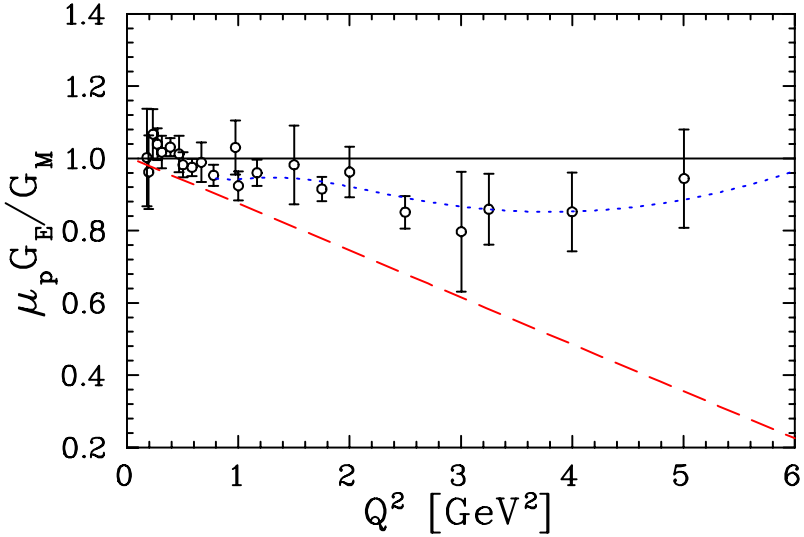

J. Arrington: nucl-ex/0305009 (2003)

- ❏ E94-110 consistent with global fit
- ❏ Rules out experimental systematics
- ❏ ϵ dependence must be large
- ❏ Unconsidered ϵ dependent radiative correction

Super–Rosenbluth, $p(e,p)$

Reduces size of dominant corrections

Rate nearly constant for protons

Reduces dominant corrections

No p dependent systematics

Sensitivity to angle momentum reduce

Luminosity monitor (second arm)

Background small

$Q^2 = 3.2$	Electron	Proton
ϵ	0.13–0.87	0.13–0.87
θ	22.2–106.0	12.5–36.3
p [GeV/c]	0.56–3.86	2.47
$\frac{d\sigma}{d\Omega}[10^{-10}\text{fm}^{-2}]$	6–340	120–170
$\frac{\delta\sigma}{\delta E}[\%/\%]$	11.5–14.2	5.0–5.3
$\frac{\delta\sigma}{\delta\theta}[\%/deg]$	3.6–37.0	5.6–19.0
Rad. Corr.	1.37–1.51	1.24–1.28

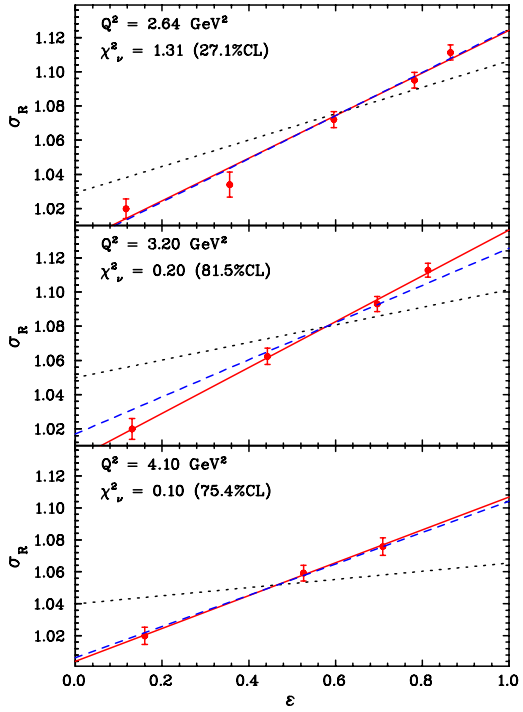

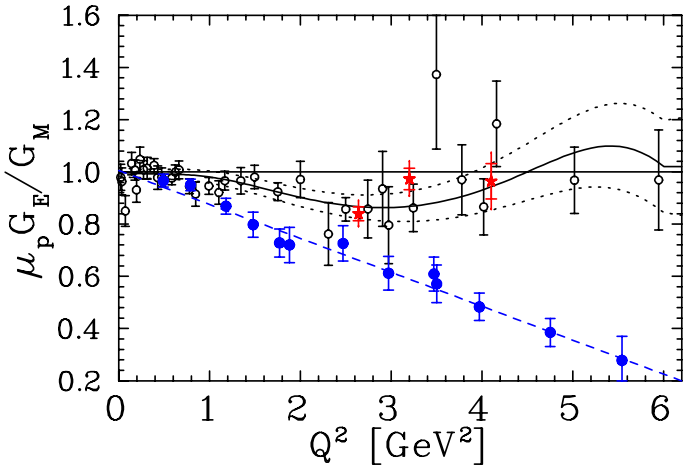

Two-Photon exchange

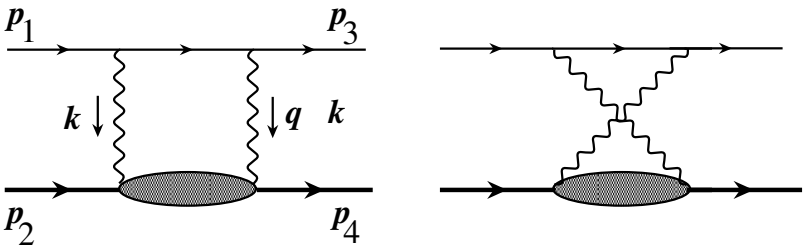

Blunden, Melnitchuk and Tjon, PRL 91, 142304 (2003), Guichon and Vanderhaeghen, PRL 91, 142303 (2003)

- Rosenbluth formula holds only for single photon exchange
- Certain two-photon processes can occur
- They are ϵ dependent and can effect the Rosenbluth extraction
- These have been calculated in the past, but are now being rexamined

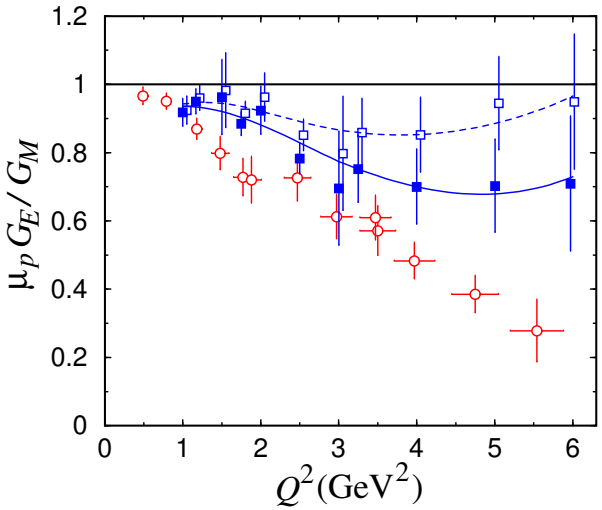

Experimental Tests:

- $\frac{\sigma(e^+p)}{\sigma(e^-p)}$
- Rosenbluth linearity
- Recoil polarization, p_n
- $\vec{p}^{\uparrow}(e,e')p$ (SSA)

Notes on two photon e^+/e^- and A_y are due to interference of the real parts of the one and two photon terms. Recoil polarization is a measure of the imaginary part

Possible to use elastic electron-nucleon scattering to observe the T-odd parity conserving target single spin asymmetry. It is time reversal odd but A_y does not violate time-reversal invariance.

$A_y = \frac{\sigma_\uparrow - \sigma_\downarrow}{\sigma_\uparrow + \sigma_\downarrow}$

Single spin asymmetry A_y arises from interference between one-photon and two-photon exchange amplitudes and is sensitive to the two-photon exhange amplitude. The normal spin asymmetry is related to the absorptive part of the elastic eN scattering amplitude. Since the one-photon exchange amplitude is purely real, the leading contribution to A_y is of order $O(e^2)$, and is due to an interference between one- and two photon exchange amplitudes.

Data and Theory

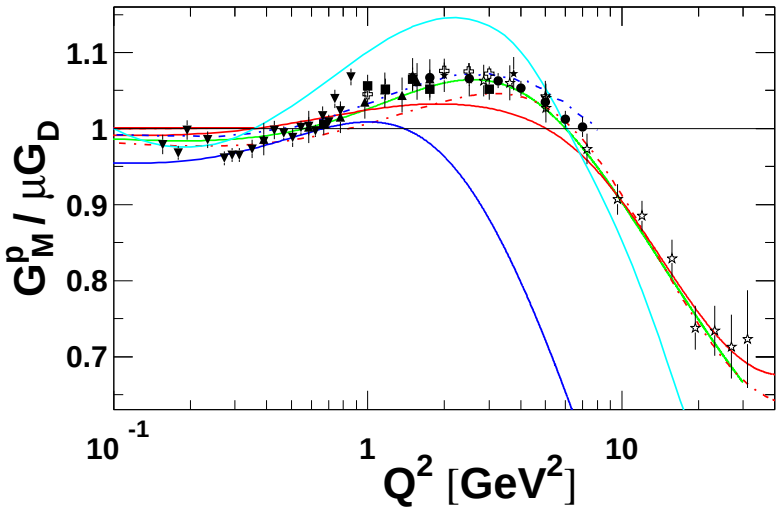

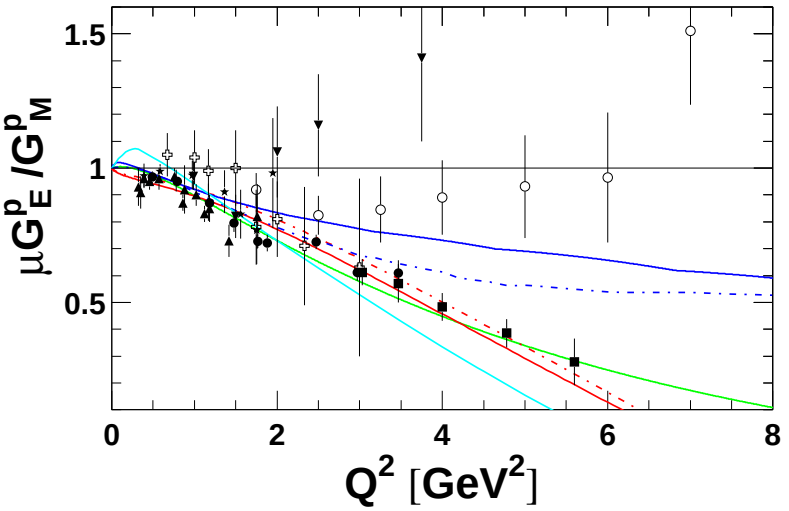

VMD + pQCD (Lomon 2002)
Soliton (Holzwarth b1)
Soliton (Holzwarth b2)
PFSA CQM GBE
LF CQM qFF (Cardarelli)
LF CQM π (Miller)

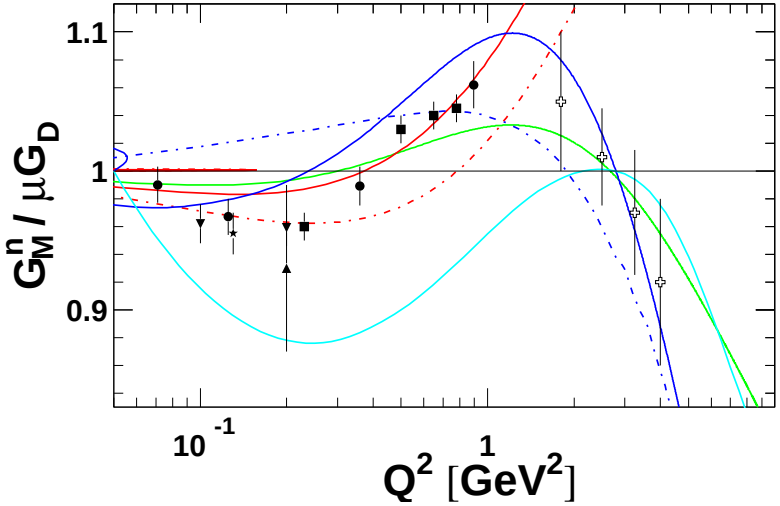

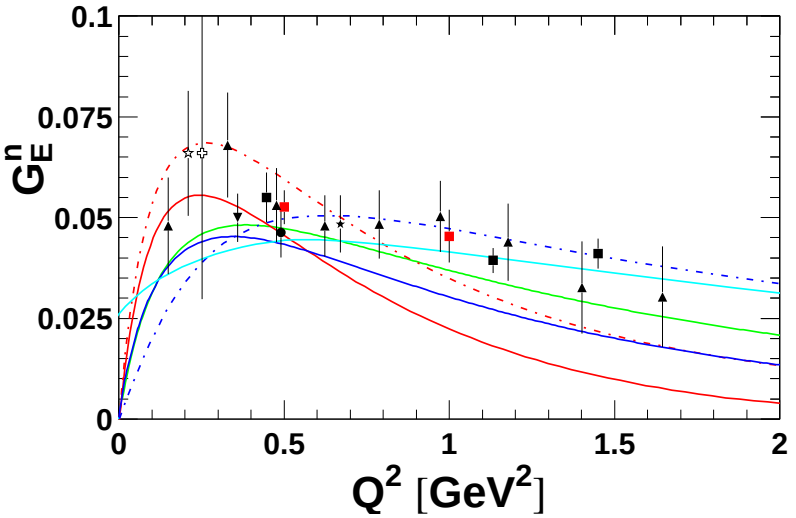

Prospects for future measurements

- Precision measurements of G_E^n out to $Q^2 = 1.5$ (GeV/c)^2 at Mami-C via $^3\overrightarrow{\mathrm{He}}(\vec{e}, e'n)$
- G_E^n via $^3\overrightarrow{\mathrm{He}}(\vec{e}, e'n)$ out to $Q^2 = 3.4$ (GeV/c)^2 in Hall A at JLAB
  - Extension to 5 (GeV/c)^2 in Hall A with 12 GeV upgrade.
- G_E^n via $^2\mathrm{H}(\vec{e}, e'\vec{n})p$ to 5 (GeV/c)^2 (proposed).
- Precision measurements up to $Q^2 \simeq 1$ (GeV/c)^2 of G_E^n and G_E^p with internal polarized targets and BLAST.
- Form factor ratio (G_E^p/G_M^p) out to 9 (GeV/c)^2 via $^1\mathrm{H}(\vec{e}, e'\vec{p})$ in Hall C at JLAB with 6 GeV beam, 2005-2006.
  - Extension out to 12.4 (GeV/c)^2 with 12 GeV upgrade.
- G_M^n out to 14 (GeV/c)^2 with an upgraded CLAS and 12 GeV upgrade.
- G_M^p to 8 (GeV/c)^2 (as part of new proposal to measure $B(Q^2)$ at 180 degrees in Hall A).

Conclusion

- Outstanding data on G_E^p out to high momentum transfer – spawning a tremendous interest in the subject and the re-evaluation of our long held conception of the proton.
- Finally G_E^n measurements of very high quality from Mainz and Jefferson Lab out to 1.5 $(\mathrm{GeV/c})^2$ exists, allowing rigorous tests of theory.
- Forthcoming data set out to large Q^2, which will further constrain any model which attempts to describe the nucleon form factors.
- A resolution of the G_E^p data from recoil polarization and Rosenbluth techniques will have applications in similar experiments from nuclei and deepen our understanding of physics and experiment.

Although the major landmarks of this field of study are now clear, we are left with the feeling that much is yet to be learned about the nucleon by refining and extending both measurement and theory. *R.R. Wilson and J.S. Levinger, Annual Review of Nuclear Science, Vol. 14, 135 (1964).*